

An Overview on IEEE 802.11bf: WLAN Sensing

Rui Du*, *Member, IEEE*, Haocheng Hua*, *Graduate Student Member, IEEE*, Hailiang Xie*, *Graduate Student Member, IEEE*, Xianxin Song, *Graduate Student Member, IEEE*, Zhonghao Lyu, *Graduate Student Member, IEEE*, Mengshi Hu, Narengerile, Yan Xin, Stephen McCann, *Senior Member, IEEE*, Michael Montemurro, Tony Xiao Han, *Senior Member, IEEE*, and Jie Xu, *Senior Member, IEEE*

Abstract—With recent advancements, the wireless local area network (WLAN) or wireless fidelity (Wi-Fi) technology has been successfully utilized to realize sensing functionalities such as detection, localization, and recognition. However, the WLANs standards are developed mainly for the purpose of communication, and thus may not be able to meet the stringent requirements for emerging sensing applications. To resolve this issue, a new Task Group (TG), namely IEEE 802.11bf, has been established by the IEEE 802.11 working group, with the objective of creating a new amendment to the WLAN standard to meet advanced sensing requirements while minimizing the effect on communications. This paper provides a comprehensive overview on the up-to-date efforts in the IEEE 802.11bf TG. First, we introduce the definition of the 802.11bf amendment as well as its formation and standardization timeline. Next, we discuss the WLAN sensing use cases with the corresponding key performance indicator (KPI) requirements. After reviewing previous WLAN sensing research based on communication-oriented WLAN standards, we identify their limitations and underscore the practical need for the new sensing-oriented amendment in 802.11bf. Furthermore, we discuss the WLAN sensing framework and procedure used for measurement acquisition, by considering both sensing at sub-7GHz and directional multi-gigabit (DMG) sensing at 60 GHz, respectively, and address their shared features, similarities, and differences. In addition, we present various candidate technical features for IEEE 802.11bf, including waveform/sequence design, feedback types, as well as quantization and compression techniques. We also describe the methodologies and the channel modeling used by the IEEE 802.11bf TG to evaluate the alternative performance. Finally, we discuss the challenges and future research directions to motivate more research endeavors towards this field in details.

Index Terms—IEEE 802.11bf, Wi-Fi sensing, WLAN sensing, DMG sensing.

I. INTRODUCTION

Over the recent 20 years, wireless fidelity (Wi-Fi®) has evolved from a nascent wireless local area network (WLAN) technology based on the family of IEEE 802.11 standards to a necessity in business and life around the world. As reported by

Rui Du, Mengshi Hu, Narengerile, Yan Xin, Stephen McCann, Michael Montemurro, and Tony Xiao Han are with Huawei Technologies Co., Ltd. (email: ray.du, tony.hanxiao@huawei.com).

Haocheng Hua, Xianxin Song, Zhonghao Lyu, and Jie Xu are with the School of Science and Engineering (SSE), the Future Network of Intelligent Institute (FNii), and the Guangdong Provincial Key Laboratory of Future Networks of Intelligence, The Chinese University of Hong Kong (Shenzhen), Shenzhen 518172, China (e-mail: haochenghua, xianxinsong, zhonghaolyu@link.cuhk.edu.cn, xujie@cuhk.edu.cn).

Hailiang Xie is with the Future Network of Intelligence Institute (FNii), The Chinese University of Hong Kong (Shenzhen), Shenzhen, China, and the School of Information Engineering, Guangdong University of Technology, Guangzhou, China (e-mail: hailiang.gdut@gmail.com).

Tony Xiao Han and Jie Xu are the corresponding authors.

*Co-first authors.

the Wi-Fi Alliance® [1], the global economic value provided by Wi-Fi reached \$3.3 trillion in 2021 and is expected to grow to nearly \$5 trillion by 2025. Besides the social and economic benefits, Wi-Fi has also led to the continuous innovation and development to enable a wide range of new services for supporting emerging applications. Among others, *WLAN sensing*, also known as *Wi-Fi sensing*¹, has recently attracted growing interests from both academia and industry.

WLAN sensing is a technology that uses Wi-Fi signals to perform sensing tasks, by exploiting prevalent Wi-Fi infrastructures and ubiquitous Wi-Fi signals over surrounding environments. In particular, Wi-Fi radio waves can bounce, penetrate, and bend on the surface of objects during their propagation. By proper signal processing, the received Wi-Fi signals can be harnessed to sense surrounding environments, detect obstructions, and interpret target movement. Thus, WLAN sensing has been successfully used in abundant residential, enterprise, indoor, and outdoor applications as shown in Fig. 1, including gesture control, fall detection, tracking, imaging, activity recognition, vital signs monitoring, etc. For instance, the Cognitive Systems Corp. released a commercial product using WLAN sensing for motion detection [2], and Origin Wireless, a start-up company, focused on the commercialization of WLAN sensing with the goal of bringing WLAN sensing to the world by partnering with key players in major verticals [3]. Therefore, WLAN sensing creates many new opportunities for Wi-Fi service providers to enter these markets.

The research on WLAN sensing can be traced back to the beginning of the 21st century, and its feasibility has been independently demonstrated by different groups in both academia and industry [4]–[10]. In general, the WLAN sensing can be classified into two main categories, which are implemented based on different wireless signal characteristics, namely the received signal strength indicator (RSSI) and channel state information (CSI), respectively. Specifically, the RSSI corresponds to the measured received signal strength at the RX² that has been widely used in the early attempts of WLAN sensing [4], [5] based on fingerprint and geometric model based methods. For example, RSSI patterns corresponding to different target locations can be used as fingerprints for

¹Wi-Fi has gradually become synonymous with WLAN due to its simplicity, reliability, and flexibility. In the 802.11 standards group, “Wi-Fi sensing” can be considered as an equivalent term of “WLAN sensing”. Therefore, this paper uses “Wi-Fi sensing” and “WLAN sensing” interchangeably.

²In fact, RSSI is a relative measure of the actual received signal strength (RSS), for which the relative magnitude can be freely defined by different chip suppliers [6]. For ease of exposition, in this paper we uniformly use RSSI to denote the actual measured received signal strength.

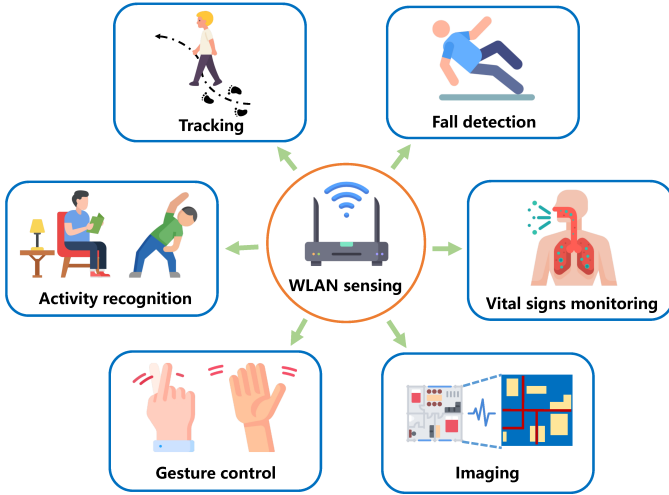


Fig. 1. Example applications of WLAN sensing.

localization [7]. By employing a simple path loss model, RSSI can also be used to estimate the distance between the transmitter (TX) and receiver (RX) [8]. In general, the RSSI-based approaches are easy to implement and with low cost. However, as the RSSIs may fluctuate significantly over time and space due to the multi-path effect in complex environments and the imperfect automatic gain control (AGC) circuit at Wi-Fi devices [11], such approaches may result in degraded sensing performance. Different from RSSI, CSI is able to provide finer-grained wireless channel information at the physical layer, which is thus considered as an alternative solution for accurate sensing [9]. CSI contains both channel amplitude and phase information over different subcarriers that provide the capability to discriminate multi-path characteristics. For instance, by processing the spatial-domain, frequency-domain, and time-domain CSI at multiple antennas, subcarriers, and time samples via fast Fourier transform (FFT), we can extract detailed multi-path parameters such as angle-of-arrival (AoA), time-of-flight (ToF), and doppler frequency shift (DFS). Other advanced super-resolution algorithms such as estimation of signal parameters via rotation invariance techniques (ESPRIT) [12], multiple signal classification (MUSIC) [13], and space alternating generalized expectation-maximization (SAGE) algorithm [14] can also be utilized to extract more accurate target-related parameters from the CSI. In various prior works [15]–[21], the CSI-based sensing approaches have been demonstrated to provide high sensing accuracy for detection and tracking.

WLAN sensing differs significantly from other existing sensing technologies based on, e.g., visible light, ultrasound, radio frequency identification (RFID), Bluetooth, and ultrawideband (UWB). In particular, visible light positioning (VLP) estimates the locations of light sensors based on the visible lights transmitted from the light-emitting diode (LED) TXs at known locations, which highly depends on the line-of-sight (LoS) channel between TXs and RXs [22]. By contrast, WLAN sensing can provide better coverage as radio signals can propagate through walls to provide additional non-LoS (NLoS) information. Furthermore, VLP needs dedicated

infrastructures such as photodetectors and imaging sensors that may lead to high system cost [31], [32], while WLAN sensing can reuse existing Wi-Fi devices with significantly lower cost. Next, ultrasound-based sensing uses an ultrasonic transceiver to record the ToF between the TX and RX, and then calculates their separation distance based on the speed of sound [33]. However, unlike Wi-Fi signals that are not harmful to health, the ultrasonic signals can be harmful to infants and pets that are sensitive to high-frequency sounds [34]. In addition, the speed of sound varies significantly with humidity and temperature (e.g., the speed of sound may increase by about 0.6 m/s for every one degree increase in temperature), thus making it less stable than WLAN sensing based on electromagnetic wave. Furthermore, RFID requires separate infrastructures to be additionally deployed [35], whereas Wi-Fi is able to leverage already available and accessible network infrastructures, which thus allow for large-scale commercial use with low cost. Moreover, RFID systems need to deploy dedicated arrays of passive RFID tags at targets, which further increases the deployment cost [25]. In addition, Bluetooth is a wireless personal area network (WPAN) technology to enable short-range wireless communication. As compared to Wi-Fi, Bluetooth has lower throughput, shorter transmission range, and needs to be deployed as a separate infrastructure, thus making the large-scale deployment of Bluetooth-based sensing difficult if not impossible. Besides, UWB positioning technologies transmit extremely short pulses over a large bandwidth (BW) (>500MHz) to track objects in a passive manner [36], which are therefore robust against multi-path issues for obtaining an accurate ToF estimation. However, the lack of large-scale infrastructure deployment limits the utilization of UWB for sensing. In summary, the comparison between the above wireless sensing technologies and WLAN sensing is listed in Table I³.

In summary, Wi-Fi has the following advantages to support various sensing applications. First of all, Wi-Fi systems are widely deployed around the world, making the commercial promotion of Wi-Fi sensing easier. Second, since sensing is incorporated as a feature of Wi-Fi, no extra sensor device is needed, thus significantly reducing the deployment and implementation cost. Third, current Wi-Fi systems have both good physical (PHY) layer features (e.g., up to 320 MHz BW at sub-7GHz, repeated field used for CSI estimation,

³Notice that cellular networks is another widely used commercial wireless technique. While there have been some prior works studying the use of existing fifth-generation (5G) systems for positioning, they primarily focus on the localization of 5G devices themselves rather than sensing the environmental objects. Only a few initial studies have explored the potential of exploiting 5G signals for sensing applications including healthcare, safety, and positioning [37], e.g., to monitor diabetic ketoacidosis (DKA), a potentially severe condition requiring hospitalization [38]. Notably, sensing is not included as a key attribute in the current 5G cellular standard and those listed work utilizing 5G signalling for sensing in [37] are mostly implemented in an ad hoc manner, as 5G systems are tailored for communication, not sensing. However, motivated by the recent advancements in WLAN sensing, the integration of sensing into cellular networks or integrated sensing and communication (ISAC) has been recognized as an important usage scenario for future sixth-generation (6G) towards IMT-2030 recently in June 2023 [39]. While cellular networks are advantageous in outdoor scenarios, WLAN sensing is more useful in indoor scenarios. 6G and WLAN sensing are expected to be complementary to each other for ubiquitous wireless sensing in the future.

TABLE I
WIRELESS TECHNOLOGIES OVERVIEW

Technology	Coverage	Power consumption	Dedicated devices	Cost	Error	Disadvantages
Visible Light	Room	1 W [22]	Yes	Moderate	≤ 7 cm [23]	Need LoS scenario
Ultrasound	Room	30 ~ 40 mW/m ²	Yes	Moderate-high	≤ 10 cm [24]	Interference
RFID	Room	10 ~ 32.5 dBm [25]	Yes	Low	≤ 15 cm [26], [27]	Response time is high
UWB	Building	-41.3 dBm/MHz [28]	Yes	High	≤ 7 cm [29]	Lack of well-developed infrastructure
Bluetooth	Building	4 dBm	Yes	Low-moderate	≤ 30 cm [30]	Limited coverage
Wi-Fi	Building	20 dBm	No	Low	≤ 20 cm [16]	Need standard modification

and multiple-input multiple-output (MIMO) with up to 8 spatial streams), and MAC layer multi-device coordination features (e.g., AP-centric architectures, mature multi-device coordination mechanism, and periodic appointment), which can be reused to facilitate WLAN sensing.

Despite the benefits and recent advancements, existing WLAN sensing works based on commercial off-the-shelf (COTS) devices still face the following key challenges, which thus motivate the development of new WLAN standards to better support WLAN sensing.

- *CSI Availability:* Although IEEE 802.11-compliant CSI extraction methods already exist, CSI is not always available at the user side in COTS Wi-Fi devices. This is because most Wi-Fi chipset manufacturers keep CSI access as a private feature and do not provide a dedicated function interface to consumers. Only a few commercial Wi-Fi devices using the outdated communication standard like 802.11n are able to access CSI data but with very limited flexibility, such as the Intel 5300 [40] and Atheros AR9580 [41] Wi-Fi cards. This has undoubtedly hindered the research and development of WLAN sensing. As a result, there is a need to identify a unified and flexible functional interface for channel measurements.
- *Transmission Adaptation:* In WLAN systems, the transceivers may dynamically change the transmission and/or reception strategies (e.g., the antenna configuration, transmit power, and the AGC levels) based on the channel conditions. If the TX and/or RX do not know *a priori* the system parameters such as the number of spatial streams, the number of antennas, and the transmit power, then the sensing measurements may become unreliable, resulting in significant performance degradation. Therefore, proper protocols to support the negotiation between transceivers are required.
- *Only Single-node Sensing Supported:* In certain scenarios, there may exist a single (or very few) access point (AP) and multiple non-AP stations (STAs), the latter of which can assist in sensing of the former. In general, their sensing collaboration can provide additional information (e.g., more signal paths as well as improved coverage) and therefore greatly improve the sensing performance. In addition, Wi-Fi devices from distinct vendors may have different sensing and computing capabilities as well as access interfaces. Through unified standardization, cooperation and interaction among multiple STAs or between APs and STAs (or even between devices from different vendors) can be exploited to enable networked sensing

and computing.

- *New Metrics and Stringent Compensation Requirements:* Conventional WLAN networks are originally designed for data transmission, without considering any sensing functionality. As such, the link throughput and latency are widely adopted performance metrics, which, however, are no longer applicable to measure the performance of WLAN sensing. Therefore, new sensing-oriented performance metrics are needed to guide the WLAN system design. In addition, received wireless signals may suffer from distortions in both amplitude and phase, and such distortions can be partially compensated via equalization for wireless communications [42]. However, the accuracy of such phase error compensation is coarse and may not meet the sensing requirements. Therefore, enhanced transmission protocol and sounding processes are necessary to improve the WLAN sensing performance, and to enable efficient and reliable ISAC [43]–[48].

To solve the aforementioned issues above, it is emerging to have new WLAN sensing standards to support sensing functionalities on Wi-Fi devices in a timely and efficient manner without significantly affecting communication performance⁴. Towards this end, IEEE 802.11 is expected to release the WLAN sensing standard amendment, i.e., IEEE 802.11bf, for WLAN sensing and ISAC. This amendment defines standardized modifications to the IEEE 802.11 PHY layer and medium access control (MAC) layer that not only enhance the sensing capability but also lead to the ease of deployment. Note that the IEEE 802.11bf amendment makes only MAC layer modifications for the sub-7GHz band, but both PHY layer and MAC layer modifications for the 60 GHz band. Specifically, IEEE 802.11bf supports the 60 GHz band sensing by improving and modifying the directional multi-gigabit (DMG) implementation in IEEE 802.11ad-2012 and the enhanced DMG (EDMG) implementation in IEEE 802.11ay-2021, both of which use beamforming to provide higher data rates. By defining specific standards support, the reliability and efficiency of WLAN sensing can be improved, thus stimulating further innovation and enabling more applications. Furthermore, the development of the standard typically results in the participation of experts from industry stakeholders. Although members from different companies have different points of interest, the sharing of information and experience can help standardize and advance the technology.

⁴Notice that previous WLAN standards from IEEE 802.11aTM-2009 to the IEEE 802.11beTM for sub-7GHz to IEEE 802.11ay-2021 for 60 GHz mainly focused on communication performance enhancement.

It is worth noting that IEEE Standardization Association previously established standards on wireless ranging, namely IEEE 802.11az [49], which was intended to address the need for a station to identify its absolute and relative positions to another station. However, IEEE 802.11az requires the object or measurement target to carry a hardware device (i.e., equipped with a cooperating device) for wireless ranging. In contrast to this, WLAN sensing focuses on device-free sensing, without requiring any devices or tags to be attached to the targets. Additionally, while IEEE 802.11az only focuses on indoor localization and positioning, WLAN sensing considers a much wider range of sensing applications beyond indoor.

In viewing of the fast development, this paper aims to provide a comprehensive and up-to-date overview on the IEEE 802.11bf standard. We first introduce the latest standardization progress, then present the detailed sensing procedure for both sub-7GHz sensing and DMG sensing, discuss the candidate technical features and simulation/channel modeling that would be adopted in IEEE 802.11bf, and finally point out the future research directions. In the literature, there have been a handful of prior works on the overview of IEEE 802.11bf [50]–[52]. For instance, [50] conducted a brief overview on IEEE 802.11bf. This work, however, fails to encompass the latest updates on IEEE 802.11bf, and does not provide the detailed DMG sensing procedure, the candidate technical features, and comprehensive future research directions as in the current paper. More recently, the authors in [51] provided a review on DMG sensing, by presenting the detailed procedures and an open-source modular simulation platform. However, this work does not discuss the important Wi-Fi sensing in sub-7GHz band, and does not present potential research directions as in this work. Besides, [52] presented a brief overview on the PHY and MAC layers specified in IEEE 802.11bf, and their interplay with the application layer by considering a specific human activity recognition task. However, this work does not address the detailed sensing procedure and does not discuss the general use cases, technical features, and future directions. As a result, this paper provides a more comprehensive overview on IEEE 802.11bf by illustrating more technical details and insights, which is expected to be a good reference for WLAN sensing and ISAC for motivating more future work along this exciting research direction.

The remainder of this paper is organized as follows and its overall structure is shown in Fig. 2. Specifically, Section II introduces how IEEE 802.11bf was formed, its definition and scope, and the timeline for its standardization. Section III presents key use cases for WLAN sensing and identifies the corresponding key performance indicator (KPI) requirements. After examining previous WLAN sensing research based on communication-oriented WLAN standards, we identify their limitations and underscore the practical need for the new 802.11bf amendment. Section IV describes the sensing procedure for both sub-7GHz sensing and DMG sensing (60 GHz) in IEEE 802.11bf to address the essential CSI acquisition problem in WLAN sensing. Specifically, we first provide a general overview of the transceiver roles and present several specific definitions. The detailed sensing procedure for sub-7GHz sensing and DMG sensing will then be illustrated,

TABLE II
SUMMARY OF MAIN ACRONYMS.

AAF	Auto Ambiguity Function
A-BFT	Association Beamforming Training
AF	Ambiguity Function
AGC	Automatic Gain Control
AID	Association Identifier
AoA	Angle-of-Arrival
AP	Access Point
AWV	Antenna Weight Vector
BFT	Beamforming Training
BI	Beacon Interval
BRP	Beam Refinement Phase
BTI	Beacon Transmission Interval
CAF	Cross Ambiguity Function
CFR	Channel Frequency Response
CIR	Channel Impulse Response
COTS	Commercial Off-The-Shelf
CSD	Criteria for Standards Development
CSI	Channel State Information
DDCH	Data-Driven Hybrid Channel Model
DFS	Doppler Frequency Shift
DMG	Directional Multi-Gigabit
EDMG	Enhanced Directional Multi-Gigabit
ESPRIT	Estimation of Signal Parameters via Rotation Invariance Techniques
FOV	Field of View
IFFT	Inverse Fast Fourier Transform
ISAC	Integrated Sensing and Communication
I-TXSS	Initiator Transmit Sector Sweep
KPI	Key Performance Indicator
LoS	Line-of-Sight
MAC	Medium Access Control
MUSIC	MUltiple SIgnal Classification
NDP	Null Data Packet
NDPA	Null Data Packet Announcement
NLoS	Non-Line-of-Sight
PAPR	Peak to Average Power Ratio
PAR	Project Authorization Request
PDP	Power Delay Profile
PHY	Physical
PPDU	Physical Layer Protocol Data Unit
RCS	Radar Cross Section
RFID	Radio Frequency Identification
RMSE	Root Mean Square Error
RSSI	Received Signal Strength Indicator
R-TXSS	Responder Transmit Sector Sweep
SAGE	Space Alternating Generalized Expectation-Maximization
SBP	Sensing by Proxy
SIFS	Short Interframe Space
SISO	Single-Input Single-Output
SLAM	Simultaneous Localization and Mapping
SNR	Signal-to-Noise Ratio
SSW	Sector Sweep
STA	Station
Sync	Synchronization
TB	Trigger-based
TCIR	Truncated Channel Impulse Response
TF	Trigger Frame
ToF	Time-of-Flight
TPDP	Truncated Power Delay Profile
TRN	Training
TRRS	Time-Reversal Resonance Strength
USID	Unassociated STA Identifier
UWB	Ultra-Wideband
Wi-Fi	Wireless Fidelity
WLAN	Wireless Local Area Network

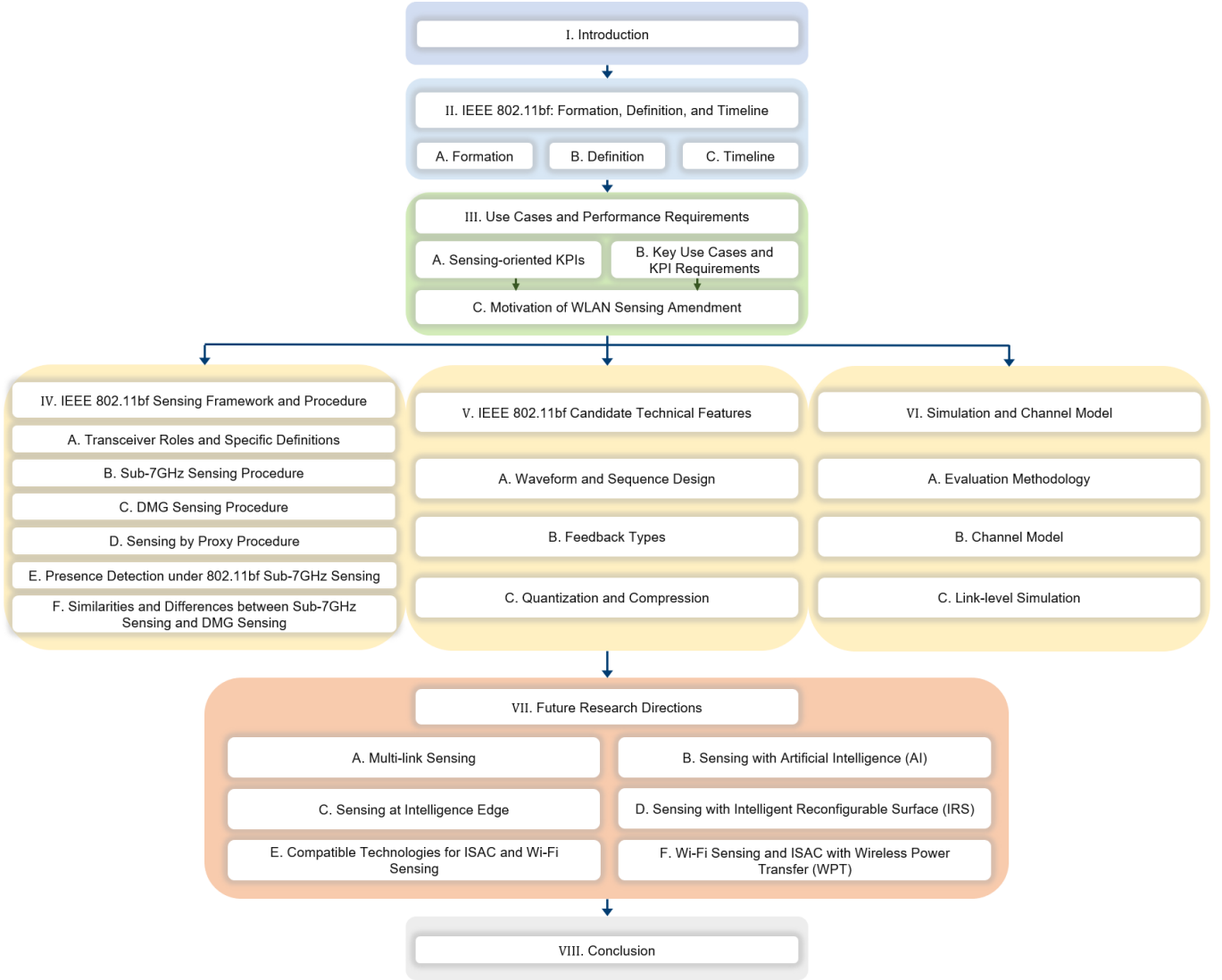


Fig. 2. The overall structure of this overview paper on IEEE 802.11bf.

respectively. The sensing by proxy procedure will be addressed after that, which is a common feature in both sub-7GHz sensing and DMG sensing. At the end of Section IV, we present a concrete example about how presence detection task is implemented under 802.11bf sub-7GHz sensing and summarize the similarities and differences between sub-7GHz sensing and DMG sensing. Section V discusses the candidate technical features for IEEE 802.11bf, including the waveform and sequence design, the feedback types, and the considered methods for quantization and compression. Section VI introduces the evaluation methodology and channel model adopted to evaluate different proposals for the IEEE 802.11bf task group. Link-level simulation, which is crucial for evaluation at a higher level, is also discussed in detail in terms of its typical setup and composition. Section VII presents the challenges and the potential future research directions along with this new 802.11bf amendment. The research endeavors towards these directions could improve the sensing performance of practical applications based on this new sensing-oriented amendment

or even provide new technical features that would possibly be included in future amendment of 802.11bf standard. Finally, Section VIII concludes this paper. For better understanding, the main terms and acronyms used in this paper are listed alphabetically in Table II. Besides, at the end of each subsequent section, we provide a brief summary and point out the lessons learned.

II. IEEE 802.11BF: FORMATION, DEFINITION, AND TIMELINE

A. Formation

The formation of a WLAN sensing project was first discussed in the IEEE 802.11 Wireless LAN Next-Generation Standing Committee (WNG SC) in July 2019 [53]–[55], where the feasibilities for WLAN to support sensing use cases and their requirements were justified. In October 2019, the WLAN sensing Topic Interest Group (TIG) was initially established. In November 2019, the formation of the WLAN sensing Study Group (SG) was approved by the New Standard Committee

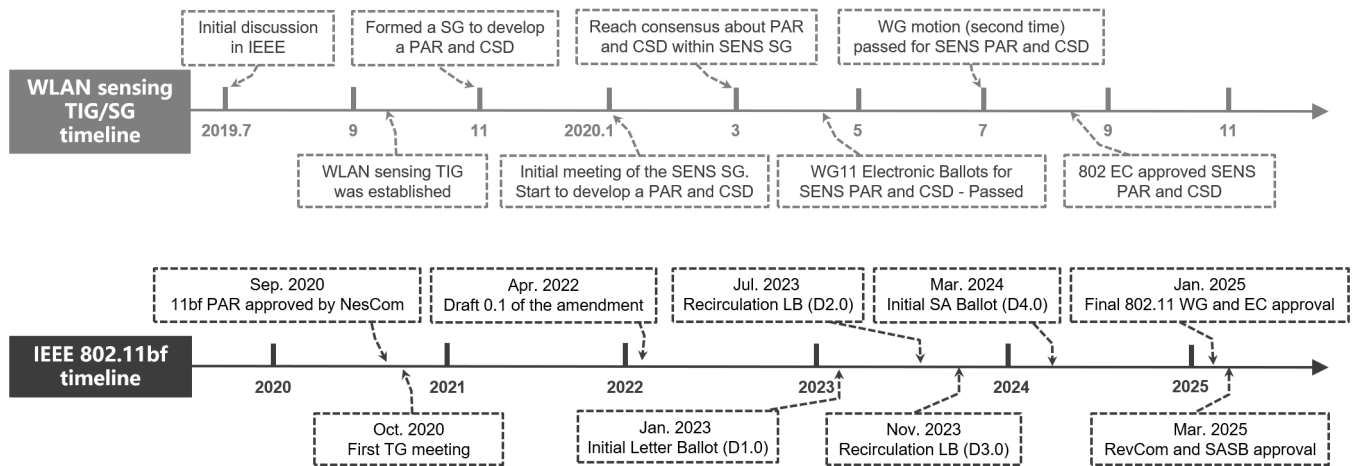


Fig. 3. Timeline and progress for the IEEE 802.11bf.

(NesCom) in the IEEE Standards Association (SA) [56]. In the WLAN sensing SG, the Project Authorization Request (PAR) and Criteria for Standards Development (CSD) were developed. Specifically, a PAR is a formal document that defines the motivation, scope, and content for a proposed standard or amendment. Moreover, it is the means by which the standards projects are started within the IEEE SA. The CSD document is an agreement between the WG and the sponsor, providing a more detailed description of the project and the requirements of the sponsor that is required by the PAR. After collaboration, consensus was reached within the WLAN sensing TIG/SG on the PAR and CSD. They were placed on the agenda of the NesCom, pending approval by the IEEE Standards Committee. With their approval of the IEEE 802.11bf PAR and CSD in September 2020, a new task group (IEEE 802.11bf) about WLAN sensing within the scope of the IEEE 802.11 working group (WG), was officially established, based on which concrete discussions towards creating an amendment for WLAN sensing begin.

B. Definition

According to the formal definition of IEEE 802.11bf, WLAN sensing refers to the use of wireless signals received from WLAN sensing capable STAs⁵ to determine the features (e.g., range, velocity, angular, motion, presence or proximity, and gesture) of the intended targets (e.g., object, human, and animal) in a given environment (e.g., room, house, vehicles, and enterprise).

As specified in the PAR, IEEE 802.11bf aims to develop an amendment that defines modifications to the IEEE 802.11 MAC as well as the DMG and EDMG PHYs to enhance WLAN sensing operation in license-exempt frequency bands between 1 GHz and 7.125 GHz and those above 45 GHz. The amendment is expected to enable backward compatibility and coexistence with existing or legacy IEEE 802.11 devices

⁵STA is a device that contains IEEE 802.11 MAC and PHY interfaces to the wireless medium (WM) [57]. For example, an STA can be an AP, a laptop, and a WLAN-enabled phone. Therefore, STAs can be mainly divided into AP STAs and non-AP STAs.

operating in the same band, by providing some basic levels of support for WLAN sensing. The IEEE 802.11bf amendment is expected to have the following features [58]:

- 1) STAs to perform one or more of the following functions: To inform other STAs of their WLAN sensing capabilities, to request and set up transmissions that allow for WLAN sensing measurements, to indicate that a transmission can be used for WLAN sensing, and to exchange WLAN sensing feedback and information;
- 2) WLAN sensing measurements to be obtained using transmissions that are requested, unsolicited, or both;
- 3) A MAC service interface for layers above the MAC to request and retrieve WLAN sensing measurements.

C. Timeline

Unlike previous amendments that focused on improving communication performance metrics such as throughput and latency, the 802.11bf amendment focuses on improving WLAN sensing performance while maintaining or improving a certain level of communication performance. Fig. 3 illustrates the timeline and progress towards the completed IEEE 802.11bf amendment. During the TIG/SG phase of this project (September 2019-September 2020), different topics (such as channel model, sequence design, and channel measurement procedure) were presented, and the proposed enhancements have been shown to be technically feasible. The first draft of the IEEE 802.11bf amendment (i.e., Draft 0.1) was released by IEEE 802.11bf in April 2022 [56]. Multiple letter ballots (i.e., technical ballots determining whether the draft of the amendment should be approved) have been or will be conducted afterward. In each ballot, IEEE 802.11 voting members can vote for or against the draft, and can optionally attach comments for revision. Submission of the draft amendment to the IEEE SA for a subsequent SA ballot is expected as early as March 2024. Finally, after the recommendation of the Standards Review Committee (RevCom) and the approval of the IEEE SA Standards Board, the project is expected to be published as an IEEE 802.11bf amendment specification in

March 2025. Actual deployment of the standard is expected to take place as early as the end of 2025.

Summary and Lessons Learned: This section discusses the details about how WLAN sensing TIG and SG is formed and the subsequent procedures to finalize the amendment for WLAN sensing. The formal definition of WLAN sensing and the corresponding terminologies are given and the general purposes, operating frequency bands, and features of IEEE 802.11bf amendment are outlined. The timeline and up-to-date progress of this amendment is also discussed. The key takeaways of this section are listed as follows.

- Experts from both industry and academia have been working on this amendment for quite a few year and the actual deployment of this standard is pending⁶.
- IEEE 802.11bf defines sensing-oriented modifications to the IEEE 802.11 MAC layer as well as the DMG and EDMG PHY layers.
- The WLAN sensing is expected to operate in 1-7.125 GHz band as well as the bands above 45 GHz.

III. USE CASES AND PERFORMANCE REQUIREMENTS

This section presents the WLAN sensing use cases and identifies the KPI requirements.

A. Sensing-oriented KPIs

In contrast to the IEEE 802.11 standards, IEEE 802.11bf requires a new variety of KPIs. In particular, a series of KPIs for WLAN sensing have been defined by IEEE 802.11bf, as described below [59].

- **Range Coverage:** The maximum allowable distance from a sensing STA to the target, within which the signal-to-noise ratio (SNR) is above a pre-defined threshold (conventionally taken as 10dB or 13dB), such that the targets can be successfully detected.
- **Field of View (FOV):** The angle through which the STA performs sensing, i.e., the FOV indicates the coverage area of a sensing device in terms of angle.
- **Range Resolution:** The minimum distance between two targets that a sensing STA can distinguish on the same direction but at different ranges.
- **Angular Resolution (Azimuth / Elevation):** The minimum angle between two targets at the same range, such that the sensing STA is able to distinguish.
- **Velocity Resolution:** The minimal velocity difference between two objects that a sensing STA can distinguish.
- **Accuracy:** The difference between the estimated range/angle/velocity of an object and the ground truth.
- **Probability of Detection:** The ratio of the number of correct predictions to the number of all possible predictions. The prediction tasks can be:
 - a) gesture detection, where a pre-defined set of gestures and/or motions shall be identified;
 - b) presence detection;
 - c) a specific body activity detection like breathing;

d) real person detection, distinguishing human beings from other objects.

- **Latency:** Expected time taken to finish the related WLAN sensing process.
- **Refresh Rate:** Frequency when the sensing refresh takes place.
- **Number of Simultaneous Targets:** The number of targets that can be detected simultaneously within the sensing area.

B. Key Use Cases and KPI Requirements

Based on the main application scenarios for WLAN sensing, IEEE 802.11bf defines a variety of use cases in [60], where the performance requirements for each use case are also outlined. For different use cases, various WLAN sensing designs have been studied to improve sensing performance.

1) *Presence Detection:* In a typical indoor scenario, reliable human presence detection is key to achieving smart home (e.g., home control). This is significant for preventing energy waste and improving the user experience. The presence detection can be mainly divided into two different states: moving (e.g., walking or making large movements) and stationary (e.g., lying, sitting, or standing still). As the variation of CSI in the time domain has different patterns for humans in different states, these patterns can be used for presence detection. In addition, some other features can be exploited to enhance the differentiation between different states, such as time-reversal resonance strength (TRRS) [61], correlation [15], higher-order moments, and Doppler spectrum. The key challenge of presence detection lies on the detection of a stationary human, which is due to the fact that the measured CSI with a stationary human is generally similar to that in empty rooms dominated by white Gaussian noise. According to [60], the maximum range coverage requirement for presence detection is 10-15 m, and specific value needs to be selected according to the room size. For example, in order to detect the presence and count the number of people in a meeting room, the maximum range coverage requirement can be generally set as 10 m. In addition, for presence detection in a multi-person environment, the range resolution, velocity resolution, and angular resolution need to be at least 0.5-2 m, 0.5 m/s, and 4-6 degrees, respectively.

2) *Activities Recognition:* Human activity recognition (HAR) plays a significant role in human-computer interaction (HCI) to help the computer understand human behaviors and intention. HAR with Wi-Fi has been used in various applications, such as fall detection, gesture recognition, and security. As the wireless channel can be distorted by human activities, we can extract patterns such as the Doppler spectrum, target speed, and amplitudes from the estimated CSI, in order to detect or to recognize human daily activities. However, there are two challenges to tackle. First, the same activity may generate different patterns at different places, since each RX can only record radial velocity of targets. Next, most existing prototype systems assumed the existence of an obvious pause between adjacent activities for segmenting them. This, however, is not true, as the human activities are usually continuous without

⁶Please refer to https://www.ieee802.org/11/Reports/tgbf_update.htm for the most updated information and progress of IEEE 802.11bf.

pause. This thus makes it challenging to automatically segment continuous activities [62]. IEEE 802.11bf allows the use of the sub-7GHz band for large motion (i.e., full-body motion) recognition and the 60 GHz band for small motion (e.g., finger and hand motion) recognition to provide higher resolution and improved recognition accuracy [60].

3) *Human Target Localization and Tracking*: Localization is the process of determining the position of a target in the region of interest, while tracking aims to confirm the trajectory of movement using the change in position of the target over time. Existing methods for indoor human target tracking/localization can be divided into two main categories, namely the fingerprinting-based and geometric model-based methods. Due to its simplicity and deployment practicability, fingerprinting-based localization [7] is one of the most widely used techniques for realizing indoor localization, but the construction of the fingerprint database is troublesome and time-consuming. Compared with fingerprinting, the geometric model-based human tracking method has better generalization in different environments. In this method, the super-resolution joint multi-parameter estimation algorithm can be adopted to improve multi-path resolution to enable human target localization and tracking [16], [17]. However, the accuracy of parameter estimation can still be limited due to the small number of antennas and limited BW. The KPI for human target localization and tracking is range accuracy within 0.2 m [60]. To support such a high range accuracy, the 60 GHz band sensing specified in IEEE 802.11bf is needed.

4) *Healthcare*: Respiration and heartbeat estimation are two common techniques to analyze human health conditions, such as sleep quality analysis [18]. By observing the vibration pattern of the phase and/or amplitude of the CSI, it is possible to estimate the respiration or heartbeat rate. Prior works such as TVS [19] and PhaseBeat [20] validated its technical feasibility. Nevertheless, estimating the respiration rate for multiple targets is still challenging. MultiSense [21] was recently proposed for estimating multiple persons' respiration rates, where the multi-person respiration sensing is treated as a blind source separation (BSS) problem. The breathing rate accuracy and pulse accuracy are the most important KPIs for respiration and heartbeat estimation. In addition, sneeze sensing has emerged as another important sensing use case, which plays a key role in transferring respiratory diseases such as COVID-19 between infectious and susceptible individuals. It is known that Doppler analysis of a spray droplets cloud is possible at high frequency (60 GHz) by calculating the volume radar cross section (RCS) for the sneeze droplets [63]. For such applications, velocity accuracy of at least 0.1 m/s is generally needed based on the Doppler frequency estimation [60].

5) *3D Vision*: Three-dimensional (3D) environment reconstruction and 3D perception of human skeletons are two typical 3D vision applications, that transform the surrounding environment and sensing targets into 3D knowledge models, respectively. Primitive methods for 3D vision are normally based on light detection and ranging (LiDARs) (e.g., simultaneous localization and mapping (SLAM)), computer vision (CV) (e.g., OpenPose API [64] for human sensing), or both. Thanks to the sparse channel brought by millimeter wave

(mmWave), several initial attempts towards building a two-dimensional (2D) map of the surrounding environment based on WLAN sensing have been conducted. For instance, a 2D range angle chart was measured in a corridor using 28 GHz mmWave by solving least square estimation problems [65]. A potential radio SLAM algorithm was proposed in [66], which is implemented via the execution of a message passing algorithm over a factor graph, where environment features are contained in collected multipath components. As for perception of human skeletons, a 3D skeleton (14 body joints) was sensed initially in [67] using radio signals (5.4-7 GHz frequency modulated continuous wave (FMCW) signals). Inspired by this, there are several follow-up items of work using CSI-based WLAN sensing and machine learning techniques to estimate 3D skeletons [68], [69]. As shown in [60], 3D vision is only applicable to the 60 GHz band, and its KPI is the accuracy of the 3D map. Towards this end, the range accuracy, velocity accuracy, and angular accuracy need to be at least 0.01 m, 0.1 m/s, and 2 degrees, respectively, which are the most demanding among all use cases.

C. Motivation of WLAN Sensing Amendment

Although a great deal of research for each use case is available, there is still a gap between their current performance and the KPIs required due to the following reasons. First, the vast majority of current research on WLAN sensing has been conducted based on existing communication standards to obtain channel measurement information, which may lead to an unstable sensing process since the frame structure and pilot design are optimized for communication instead of sensing. Second, as previous standards are communication-oriented, most devices from different vendors operating on these WLAN standards do not provide easily accessible and unified interfaces to efficiently obtain the CSI for sensing applications. In particular, in current WLAN sensing research, the CSI acquisition is implemented for different use cases in an ad hoc manner. As a result, devices from different vendors might run the same sensing application under different parameters and constraints. Furthermore, such implementations also lead to a lack of negotiation and cooperation among multiple STAs involved in sensing, making it difficult to further improve the sensing diversity and correspondingly enhance the performance of various sensing tasks. The lack of coordination might also affect the communication functionality.

To overcome the above limitations, the 802.11bf standard is developed to define unified and standardized WLAN sensing-specific operations, and thus maximize the features, efficiencies, and capabilities of WLAN sensing for improving the sensing performance to meet the KPI requirements. The 802.11bf standard not only enables sensing STAs to behave in a specific and deterministic way, but also enables the network to operate jointly to support the aforementioned key use cases. Furthermore, the advent of 802.11bf provides a platform to enable various innovative sensing algorithms. Last but not least, previous implementation of these use cases mostly operates in mid-band WLAN standards. However, to facilitate the high-resolution and high-accuracy requirements

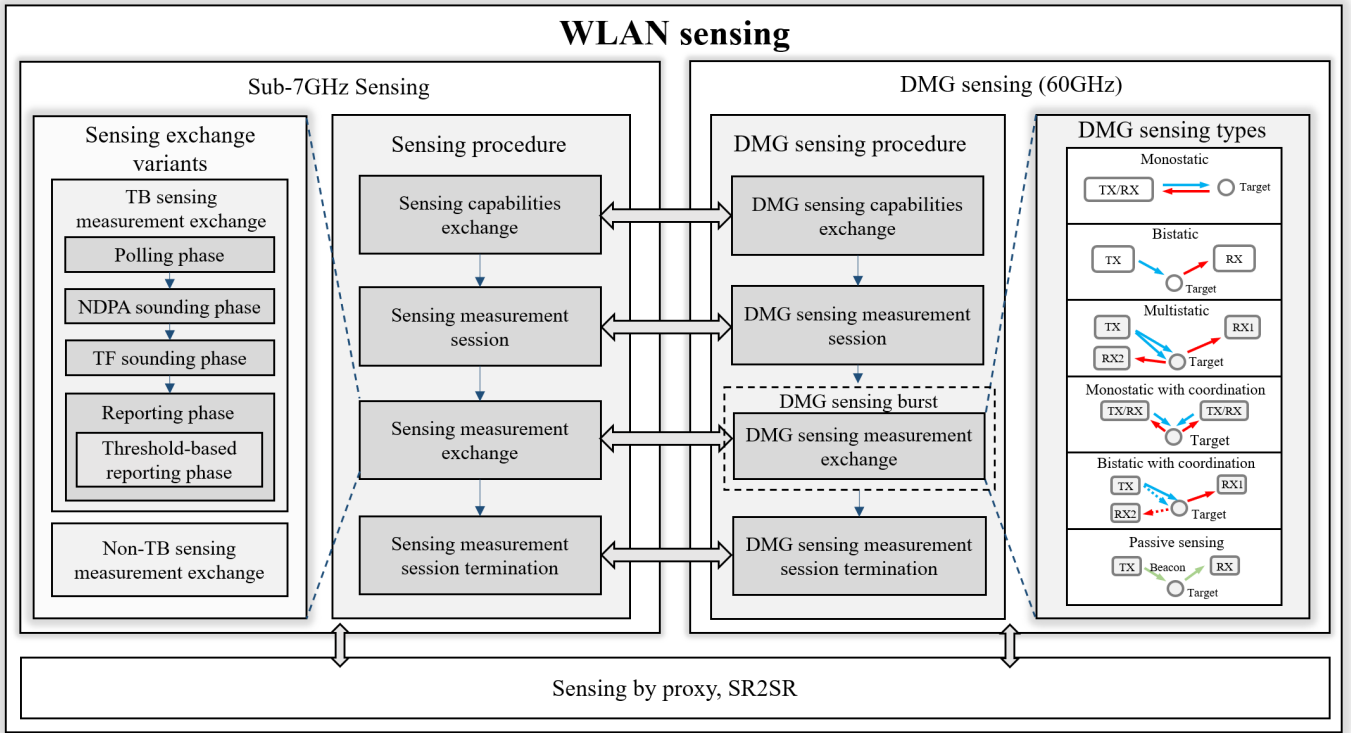


Fig. 4. General overview of WLAN sensing procedure for both sub-7GHz sensing and DMG sensing.

for these sensing applications, it is essential to specify high-band DMG sensing in WLAN standards.

Summary and Lessons Learned: In this section, we first formally define a set of sensing-oriented KPIs. After that, we discuss several key use cases including presence detection, activities recognition, human target localization and tracking, healthcare, and 3D vision. For each use case, we review those previous works based on communication-oriented WLAN standards and specify their expected KPI requirements. It is clear that there still exists a gap between the current performance and their expected KPIs in each use case, which motivates the amendment for WLAN sensing. The key takeaways are the underlying rationale and benefits of this amendment, which are listed as follows.

- Stable sensing process with accessible and unified interfaces for efficient CSI acquisition.
- More negotiation and cooperation among different STAs (i.e., enabling network sensing) for enhanced sensing and communication performance.
- Providing a platform for innovative sensing algorithms validation.
- Standardizing high-band DMG sensing for applications with high resolution and accuracy requirements.

IV. IEEE 802.11BF SENSING FRAMEWORK AND PROCEDURE

From a standardization perspective, the most essential issue to be dealt within IEEE 802.11bf is measurement acquisition, where the goal is to obtain sensing measurements from an IEEE 802.11-based radio. Since different use cases require

different requirements, 802.11bf defines two different sensing measurement acquisition procedures that can operate in the sub-7GHz and 60 GHz bands, respectively. For ease of exposition, in the sequel, we refer to 60 GHz sensing as DMG sensing. As the DMG sensing additionally implements the directional beamforming, more sophisticated design is required. In this section, we first introduce the basic IEEE 802.11bf definition for a sensing STA and then provide details of the two sensing procedures to explain how measurement acquisition is achieved. A general overview of WLAN sensing procedure for both sub-7GHz sensing and DMG sensing is shown in Fig. 4. For sensing in both sub-7GHz and 60 GHz band, the overall sensing procedure can be similarly classified into four parts in general, i.e., sensing capabilities exchange, sensing measurement session, sensing measurement exchange (DMG sensing burst composed of a bunch of DMG sensing measurement exchanges), and sensing measurement session termination. However, sensing in these two different frequency bands are quite different in terms of sensing measurement exchange variants. For sub-7GHz sensing, two variants are incorporated, namely trigger-based (TB) sensing measurement exchange and non-TB sensing measurement exchange, respectively. Each TB sensing measurement exchange is composed of the following sequential phases, including the polling phase, null data packet announcement (NDPA) sounding phase, trigger frame (TF) sounding phase, and reporting phase. Furthermore, each DMG sensing measurement exchange is generally classified into the following categories, i.e., the monostatic, bistatic, multistatic, monostatic with coordination, bistatic with coordination, and passive sensing. In addition, as it is possible that a STA might

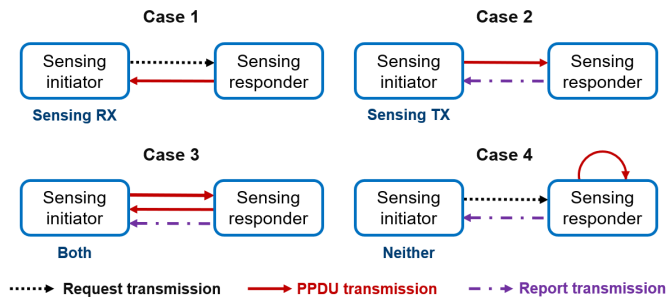


Fig. 5. Sensing configuration for IEEE 802.11bf.

not be able to finish the whole sensing process on its own, sensing by proxy procedure is outlined in IEEE 802.11bf to allow a non-AP STA to request an AP to perform WLAN sensing on its behalf over both frequency bands. The following subsections will illustrate a more detailed packet exchange process and elaborate expositions of the aforementioned concepts and procedures for each sensing frequency band.

A. Transceiver Roles and Specific Definitions

To start with, the sensing initiator and sensing responder are defined depending on which STA initiates a WLAN sensing procedure, and requests and/or obtains measurements. A sensing initiator is a STA that initiates a sensing procedure, while a sensing responder is a STA that participates in a sensing procedure initiated by a sensing initiator. Both the sensing initiator and sensing responder can be an AP or a non-AP STA (i.e., client).

On the other hand, depending on who transmits the IEEE 802.11-based signal (i.e., physical layer protocol data unit (PPDU)⁷) to obtain measurements, we have two other types of roles, namely sensing TX and sensing RX. Specifically, a sensing TX is a STA that transmits PPDU used for sensing measurements in a sensing procedure, and a sensing RX is a STA that receives PPDU sent by a sensing TX and performs sensing measurements in a sensing procedure. The ability to define the role of each STA as sensing TX or sensing RX is an important feature of WLAN sensing.

It is noticed that a sensing initiator can be either a sensing TX or a sensing RX, both or neither, during a sensing procedure. The sensing responder is similar to the sensing initiator and can be either the sensing TX, the sensing RX or both. In addition, a STA can assume multiple roles in one sensing procedure. Taking the sensing initiator as an example, the sensing configuration used by WLAN sensing can be roughly divided into four cases, as shown in Fig. 5, which are explained in the following.

- In the first case, the sensing initiator is the sensing RX, which directly obtains measurements by itself using PPDU transmitted by the sensing responder.
- In the second case, the sensing initiator is the sensing TX, which transmits PPDU and performs the sensing

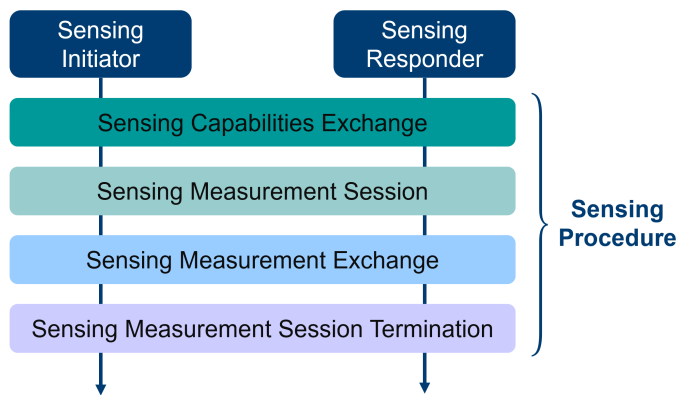


Fig. 6. Overview of the sub-7GHz sensing procedure.

function by using the feedback of measurements from the sensing responder.

- In the third case, the sensing initiator is both a sensing TX and a sensing RX, which can obtain uplink measurements by receiving PPDU and obtain downlink measurements through feedback.
- Finally, the sensing initiator is neither a sensing TX nor a sensing RX. In this case, the sensing responder feeds back the measurements obtained by other means to the sensing initiator, thus allowing the sensing initiator to obtain the measurements without sensing PPDU.

B. Sub-7GHz Sensing Procedure

A main contribution of the IEEE 802.11bf amendment will be the specification of procedures that allow for WLAN sensing applications to reliably and efficiently obtain measurement results. Specifically, through the sensing procedure, IEEE 802.11bf can provide a service that enables a STA to obtain sensing measurements of the channel between two or more STAs and/or the channel between a receive antenna and a transmit antenna of a STA. The framework basis of the IEEE 802.11bf WLAN sensing procedure for sub-7GHz systems is illustrated in Fig. 6. Specifically, a sub-7GHz sensing procedure typically contains four phases, namely the sensing capabilities exchange, sensing measurement session, sensing measurement exchange, and sensing measurement session termination. Note that IEEE 802.11bf standardization is ongoing. In the following, details of the general sub-7GHz sensing procedure which have been developed in IEEE 802.11bf so far are introduced.

- *Sensing Capabilities Exchange*: At this stage, the sensing capable devices exchange their sensing capabilities. Sensing capabilities exchange is performed during the association phase for associated stations and is performed before the association phase for unassociated stations.
- *Sensing Measurement Session*: Sensing measurement session allows for a sensing initiator and a sensing responder to exchange and agree on operational attributes (i.e., special operational information) associated with a sensing measurement exchange, which includes the role of the STA, the type of measurement report, and other operational parameters. To identify a specific set of operational

⁷It is noticed that a PPDU is a data unit exchanged between two peer PHY entities to provide the PHY data service.

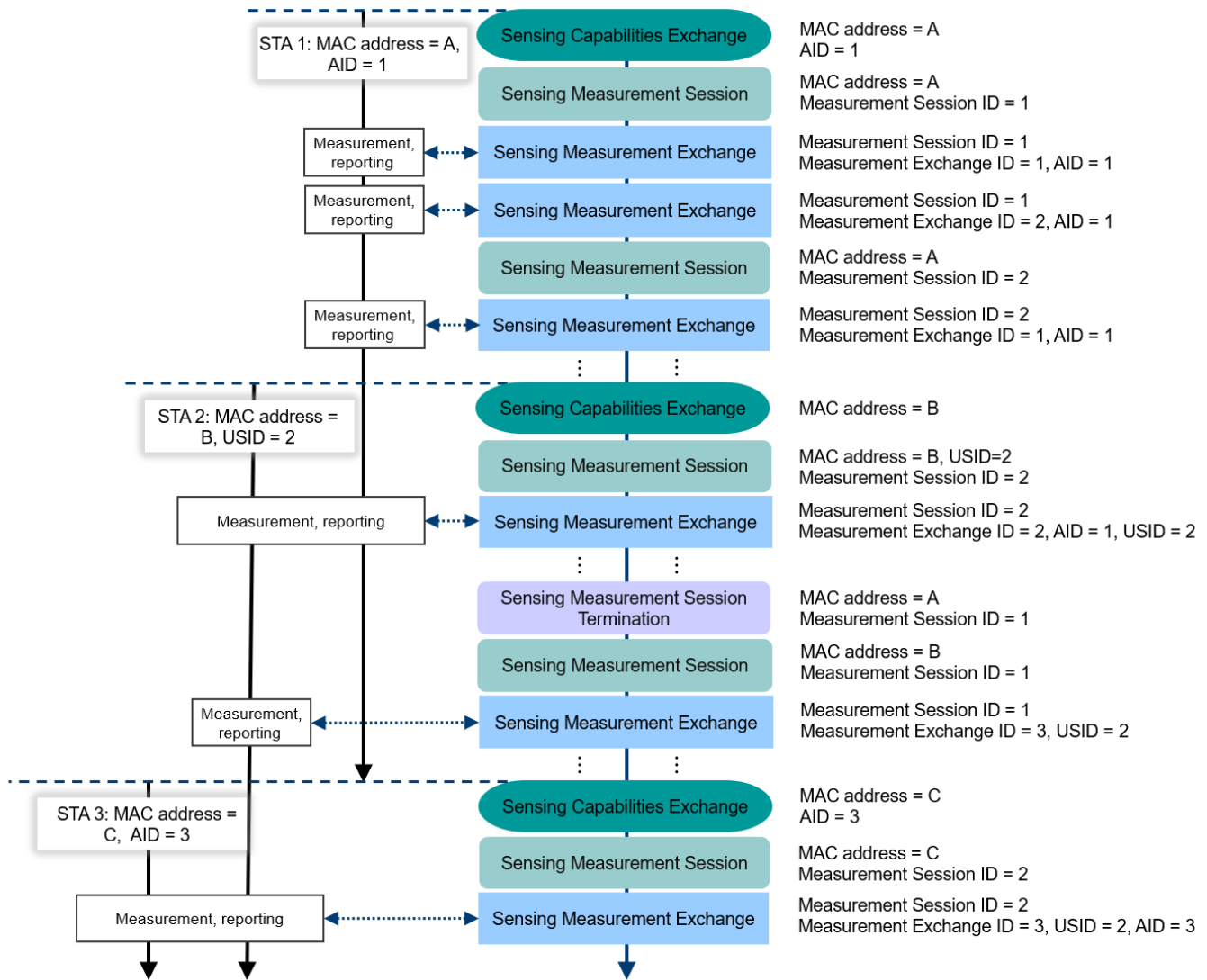


Fig. 7. Example of sub-7GHz sensing procedure.

attributes, measurement sessions with different sets of operational attributes are assigned by different Measurement Session IDs.

- *Sensing Measurement Exchange*: In the sensing measurement exchange, sensing measurements are performed. The Measurement Exchange IDs may be used to identify different sensing measurement exchanges.
- *Sensing Measurement Termination*: In the sensing measurement termination, the corresponding sensing measurement sessions are terminated. The sensing initiator and the sensing responder release the allocated resources to store the sensing measurement session.

An example of the general sub-7GHz sensing procedure is shown in Fig. 7, where an AP performs sub-7GHz sensing with three non-AP STAs, which are referred to as STA 1, STA 2, and STA 3 with MAC addresses A, B, and C, respectively. STA 1 has AID 1, STA 2 has USID 2, and STA 3 has AID 3. The example starts with a sensing capabilities exchange procedure performed between the AP and STA 1, which exchange the

detailed sensing capabilities supported by the AP and STA 1 (AID 1). A first sensing measurement session procedure is then performed, which defines a set of operational attributes labeled with a Measurement Session ID equal to 1. After the sensing measurement session, sensing measurement exchanges are performed based on the defined operational attribute set (Measurement Session ID equal to 1). Each measurement exchange is labeled with a Measurement Exchange ID. After some time, a second sensing measurement session procedure is performed between the AP and STA 1, which defines a second operational attribute set that is labeled with a Measurement Session ID of 2. After the second sensing measurement session, any subsequent sensing measurement exchanges may be performed based on either the first (Measurement Session ID equal to 1) or the second (Measurement Session ID equal to 2) operational attribute sets. An operational attribute set may be terminated by performing a sensing measurement session termination procedure. For example, Measurement Session ID equal to 1 is terminated for the sensing session between the

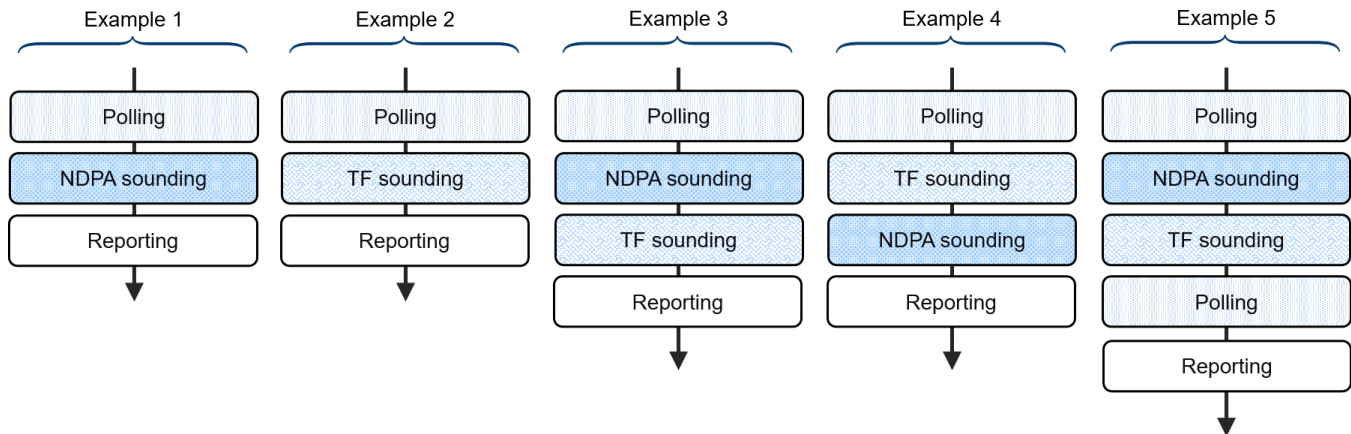


Fig. 8. Examples of possible TB sensing measurement instances.

AP and STA 1.

Among the four major steps in the general sub-7GHz sensing procedure, the sensing measurement exchange deserves further investigations. Depending on whether there exist trigger frames in the sensing measurement procedure, two broad measurement configurations are defined, i.e., TB configuration and non-TB configuration. Accordingly, a specific sensing measurement exchange can be one of the two options, i.e., a TB sensing measurement exchange or a non-TB sensing measurement exchange, which are elaborated more in the following.

1) *TB Sensing Measurement Exchange*: The TB sensing measurement exchange is a trigger-based variant of the sensing measurement exchange for the case where the AP is the sensing initiator, and one or more non-AP STAs are the sensing responders. It may comprise a polling phase, null data packet (NDP)⁸ announcement sounding phase, TF sounding phase, and reporting phase. Note that any combination in the order of these phases may be present in the TB sensing measurement exchange, as shown in Fig. 8. To effectively measure the channel between the initiator and multiple responders, the initiator AP should first perform polling to identify the responder STAs that are expected to participate in the upcoming sensing sounding in the TB sensing measurement exchange. If STAs are likely to perform upcoming sensing sounding, they can return a response to request participation in a TB sensing measurement exchange. Polling should always be performed to check the availability of the responder STA before performing the actual sensing measurement in the TB sensing measurement exchange. After the polling for sensing, the initiator AP can then perform sensing measurement with the responder STAs. In the NDPA sounding phase, the initiator AP, which is a sensing TX, sends an NDP to the STAs that are sensing RXs and that have responded in the polling phase to perform downlink sensing sounding. In the TF sounding phase, the initiator AP, as a sensing RX, requests the responder STAs, which are sensing TXs and respond in the polling phase, to perform NDP transmission for uplink sensing sounding. It

is noticed that both NDPA sounding phase and TF sounding phase are optionally present, and will only be present if at least one responder STA that is a sensing RX/TX has responded in the polling phase. The last phase of a TB sensing measurement exchange is the reporting phase.

Fig. 9 shows an example of a TB sensing measurement exchange consisting of a polling phase, an NDPA sounding phase, and a TF sounding phase. In the polling phase, the AP polls five STAs, where STA 1 and STA 2 are sensing TXs and STA 3, STA 4, and STA 5 are sensing RXs. STA 1-STA 4 return responses (e.g., Clear to send (CTS)-to-self) to the AP, so both a TF sounding phase and NDPA sounding phase are present. In the TF sounding phase, the AP sends a Sensing Sounding Trigger frame to STA1 and STA 2 to solicit Sensing Responder to Sensing Initiator (SR2SI) NDP transmissions. In the NDPA sounding phase, the AP sends a Sensing NDP Announcement frame followed by Sensing Initiator to Sensing Responder (SI2SR) NDP to STA3 and STA 4. There is a short interframe space (SIFS) between each frame.

In the reporting phase, sensing measurement results are reported, and the corresponding sensing measurement reporting can be either immediate or delayed. During the reporting phase, the TX AP sends a trigger frame to the RX STAs to request sensing measurement results obtained from the SI2SR NDP of the current measurement exchange when an immediate feedback reporting is provided, or from the SI2SR NDP of the previous measurement exchange when a delayed feedback reporting is provided. For the delayed reporting, a responder STA can send delayed measurement reports for multiple sensing measurement sessions together as a single feedback.

Moreover, IEEE 802.11bf also provides an optional threshold-based reporting phase in the TB sensing measurement exchange. It is applicable in the case where the sensing initiator of the TB sensing measurement exchanges is a sensing TX. The optional threshold-based reporting phase consists of a CSI variation reporting subphase and possibly a measurement reporting subphase. The CSI variation represents the quantified difference between the currently measured CSI and the previously measured CSI at the sensing RX. The CSI variation

⁸A NDP is a special PPDU that includes a preamble portion but no payload.

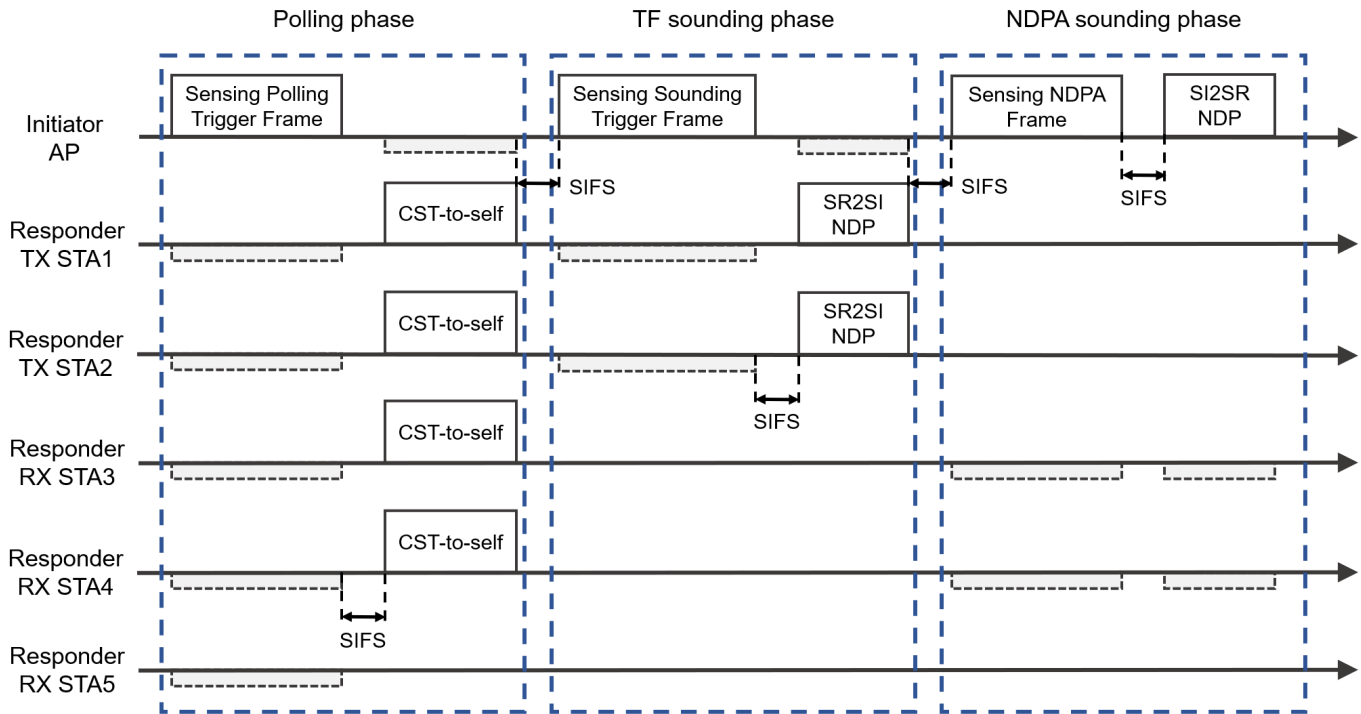


Fig. 9. Example of TB sensing measurement exchange.

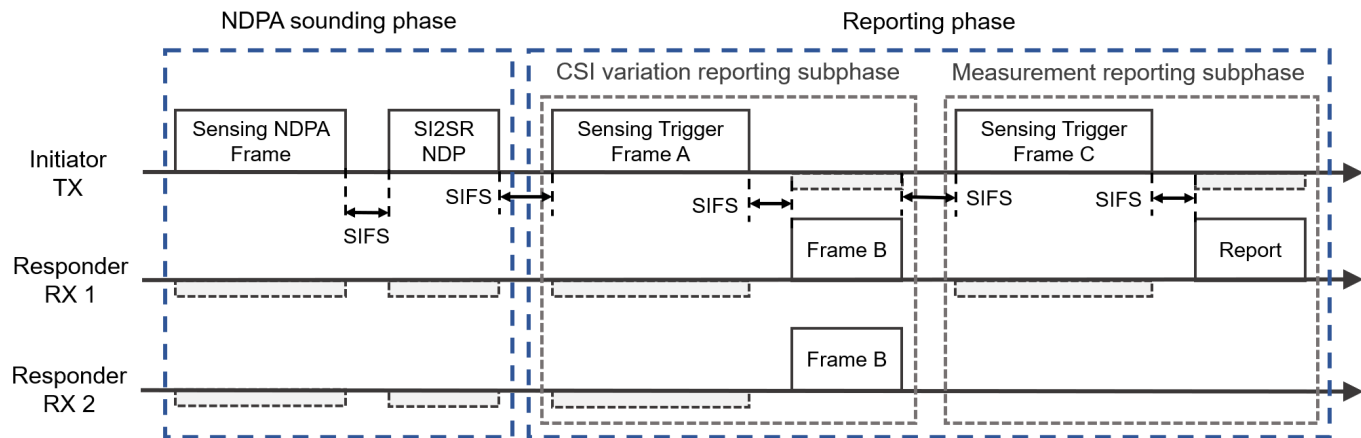


Fig. 10. Example of threshold-based reporting phase in a TB sensing measurement exchange.

threshold to be compared to the CSI variation value for each sensing responder, is determined by the sensing initiator, and different sensing responders have different thresholds. In the CSI variation reporting subphase, after receiving the trigger frame from the sensing initiator, the sensing responder shall send the CSI variation feedback value (in frame B) to the initiator for threshold comparison. In the measurement reporting subphase, only sensing responders with CSI change values greater than or equal to the CSI change threshold assigned to them are required to provide feedback on the measurement results. An example of the threshold-based reporting phase in a TB sensing measurement exchange is shown in Fig. 10.

2) *Non-TB Sensing Measurement Exchange*: The non-TB sensing measurement exchange is a non-trigger-based variant

of the sensing measurement exchange for the case where a non-AP STA is the sensing initiator, and an AP is the sensing responder. In the non-TB sensing measurement exchange, when the initiator STA is both a sensing TX and a sensing RX, it first sends a Sensing NDPA frame to the responder AP to configure the parameters for the subsequent SI2SR NDP and SR2SI NDP. Then, after going through an SIFS, an SI2SR NDP is sent to perform uplink sensing sounding. Upon correct reception of the NDPA frame, the responder AP send an SR2SI NDP as a response to the initiator STA to perform downlink sensing sounding. Sensing feedback for the SI2SR sounding can be sent to the initiator STA after the SR2SI NDP transmission. When the initiator STA is the sensing TX, sensing detection is performed only during SI2SR

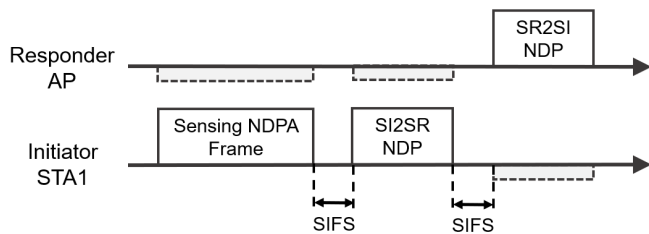


Fig. 11. Example of non-TB sensing measurement exchange.

NDP transmission, while the SR2SI NDP is continued to be sent by the responder AP as an acknowledgment of the receipt of the sensing NDP frame and the SI2SR NDP. In this case, the SR2SI NDP will be transmitted at the minimum possible length. When the initiator STA is the sensing RX, SR2SI NDP is responsible for the sensing detection while SI2SR NDP is transmitted at the minimum possible length to maintain a unified flow. More details can be found in [70]. An example of the non-TB sensing measurement exchange is shown in Fig. 11.

C. DMG Sensing Procedure

IEEE 802.11ad and IEEE 802.11ay make full use of beamforming at the 60 GHz band in the (E)DMG implementations to compensate for the severe path loss, and provide multi-Gigabit-per-second data-rate throughput. IEEE 802.11bf extends these techniques to cope with the challenges of sensing in the mmWave band, and designs an efficient sensing procedure, denoted as DMG sensing procedure. The DMG sensing procedure is an improved version of the general WLAN sensing procedure to support highly directional sensing in the 60 GHz band. As opposed to sub-7GHz sensing, DMG sensing offers wider channel BW and smaller wavelength (allowing the use of compact antenna arrays for beamforming), thus enabling higher range resolution and angular resolution. Depending on the number and roles of the devices involved in sensing, there are various types of DMG sensing, including monostatic, bistatic, multistatic, monostatic sensing with coordination, bistatic sensing with coordination, and passive sensing, as shown in Fig. 12. Different DMG sensing types have different sensing processes, which will be described in detail later. By incorporating innovative sensing techniques and procedures in the frequency band range around 60 GHz, IEEE 802.11bf enables more accurate sensing applications.

As shown in Fig. 13, a DMG sensing procedure generally comprises a DMG sensing capabilities exchange, DMG sensing measurement session, DMG sensing burst, DMG sensing exchange, and DMG sensing measurement session termination. In particular, a DMG sensing burst is a virtual concept that defines a set of multiple DMG sensing exchanges in order to perform Doppler estimation in each burst. IEEE 802.11bf specifies the time between consecutive exchanges in a DMG sensing burst as the intra-burst interval, and the time between consecutive bursts as the inter-burst interval. Note that the DMG sensing procedure is a subset of the WLAN sensing procedure, so the rules for WLAN sensing procedure also apply to DMG sensing procedure unless otherwise stated.

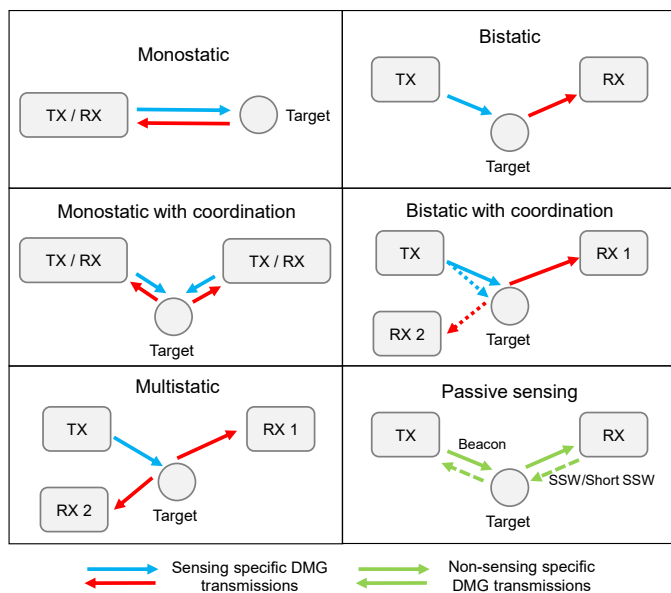


Fig. 12. Examples of different DMG sensing types.

Prior to the DMG sensing procedure, it is assumed that beamforming training between the sensing initiator and the sensing responder(s) is completed in advance, which facilitates the exchange of preamble, data, and synchronization information between them in the DMG sensing procedure. At the beginning of the DMG sensing procedure, DMG sensing capabilities are exchanged between the sensing initiator and the sensing responder to identify the type of DMG sensing. Then, a set of operational attributes associated with DMG sensing bursts and DMG sensing exchanges are defined in the DMG measurement session, which may include intra-burst and inter-burst schedule, roles of the sensing initiator and sensing responder, and other parameters. After the setup of the DMG sensing session procedure, DMG sensing exchanges are performed based on the defined operational attribute set to perform channel measurements. A DMG sensing exchange typically contains three phases, i.e., initiation phase, sounding phase, and reporting phase. It is worth noting that only the sounding phase is mandatory, while the initiation and reporting phases are optional. According to different DMG sensing types, the specific implementation of DMG measurement exchanges will be different. More details are given as follows.

1) *Monostatic Sensing*: In monostatic sensing, any IEEE 802.11-compatible PPDU suitable for sensing can be transmitted by a monostatic (E)DMG STA. Since the sensing TX and sensing RX are the same STA, there is no need for interoperability with any uninvolved STAs. When an uninvolved STA receives a standard compliant signal transmitted by a monostatic (E)DMG STA, the PPDU may be measured at the PHY layer, but will be discarded at the MAC layer because the frame is not addressed to it.

2) *Bistatic Sensing*: In bistatic sensing, the sensing TX and the sensing RX are two distinct STAs. The bistatic DMG sensing exchange consists of a number of Beam Refinement Phase (BRP) frames with a training (TRN) field transmitted by the sensing TX and one BRP frame sent by the sensing

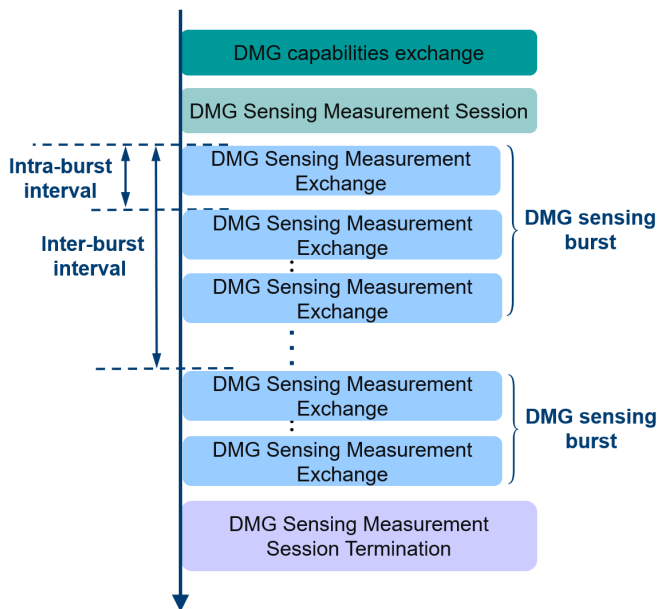


Fig. 13. Example of DMG sensing procedure.

RX, as shown in Fig. 14. IEEE 802.11bf reuses the IEEE 802.11ay beamforming training (BFT) method during a DMG sensing exchange by using the TRN field appended to the end of the BRP frames. The TRN field is composed of a series of TRN subfields. The first P TRN subfields are responsible for synchronization and channel estimation, where the sensing TX uses the same antenna weight vector (AWV) configuration towards the sensing RX as the data field. Note that the AWV is a vector of weights imposed on each element of an antenna array that enables the energy of the beam to be concentrated in a narrow range and emitted in a certain direction, i.e., beamforming. In the next M TRN subfields, the AWV may be changed in each TRN subfield to sweep through all the beams to cover the sensing environment. The initiator shall choose the format of the TRN field in each of the transmitted BRP frames in a way that it is compatible with the responder capabilities, such as BRP-TX, BRP-RX, or BRP-RX/TX PPDU. For the case where the sensing initiator is the sensing TX, the initiator transmits the BRP frames with the TRN field during the sounding phase, and the responder receives these frames and performs the sensing measurements on the TRN fields. In the reporting phase, the responder responds with a BRP frame containing the report as channel measurement feedback. For the case where the sensing initiator is the sensing RX, the initiator first transmits a BRP frame. Then, BRP frames with a TRN field are transmitted by the responder. There is no reporting phase in the receive initiator DMG bistatic measurement exchange since the sensing initiator is the sensing RX. In particular, if the DMG sensing subfield in the BRP request field is equal to 1, it indicates that the PPDU of the current BRP frame is for sensing and will not be used for beamforming training. At this point, the BRP frames sent by the sensing initiator will contain the BRP Sensing element in which the control and management parameters necessary for initiating the sensing exchange are set.

3) *Multistatic Sensing*: In multistatic sensing, the sensing TX and more than one sensing RXs are distinct STAs. Multistatic sensing is significantly different from bistatic sensing because the preamble/data field of the existing PPDU is only for a specific STA, while other STAs may not receive it, if the PPDU is transmitted with the same AWV as the data field. Furthermore, multiple devices need to be synchronized to a single time base. Thus, an initiation phase of multistatic EDMG sensing exchange is needed to prepare the different responder STAs for the measurement, and to schedule the synchronization and the TRN field. To enable multiple RXs to participate in sounding using the same PPDU (i.e., EDMG Multi-static Sensing PPDU), IEEE 802.11bf allows multiple synchronization (Sync) fields to be inserted after the EDMG-short training field (EDMG-STF) (if present) or the EDMG-Header-A to replace the EDMG-channel estimation field (EDMG-CEF) and data fields of the PPDU to ensure synchronization of the different RXs. A padding field ensures that the length of the Sync fields together is equal to a multiple of the TRN-Unit length. The TRN field of an EDMG Multi-Static Sensing PPDU is identical to the TRN field of an EDMG PPDU, with the exception that multiple TRN-Unit P subfields are transmitted with the AWV to the respective RXs. Fig. 15 illustrates a DMG sensing exchange of multistatic sensing. The handshake between the initiator and the responders activates the responders to be ready to participate in the sounding and report in sequence during the reporting phase. After receiving the response from the last responder, the initiator transmits the EDMG Multistatic Sensing PPDU for synchronization and DMG sensing purposes. In particular, the sensing responders STA 1 and STA 2 are synchronized with the initiator using the corresponding Sync fields. In the reporting phase, the sensing initiator polls each of the responders for a sensing report, and the sensing responders respond in the predefined order.

4) *Monostatic Sensing with Coordination*: Monostatic sensing with coordination is an extension of monostatic sensing, where the transmissions of one or more devices performing monostatic sensing is coordinated by a sensing initiator. The sensing initiator with the coordinated monostatic sensing can be a STA involved in sensing measurements or a STA that does not have monostatic sensing capability. Similar to multistatic sensing, there is a need to coordinate multiple monostatic devices, so scheduling and control information is exchanged between the sensing initiator and all sensing responders during the initiation phase. In coordinated monostatic sensing mode, the sensing initiator may request the sensing responders to transmit and receive a monostatic PPDU in a specific direction by indicating the TX/RX beams to be used in each measurement burst. IEEE 802.11bf specifies that the sounding for each responder can be performed either sequentially or simultaneously. In monostatic sensing with coordination, each collaborating STA only uses its own clock to transmit and receive sensing signals, so there is no need to synchronize between different STAs as in multistatic sensing. This greatly reduces the synchronization overhead.

5) *Bistatic Sensing with Coordination*: Bistatic sensing with coordination is an extension of the bistatic sensing to coordinate multiple sensing responders by one sensing initiator.

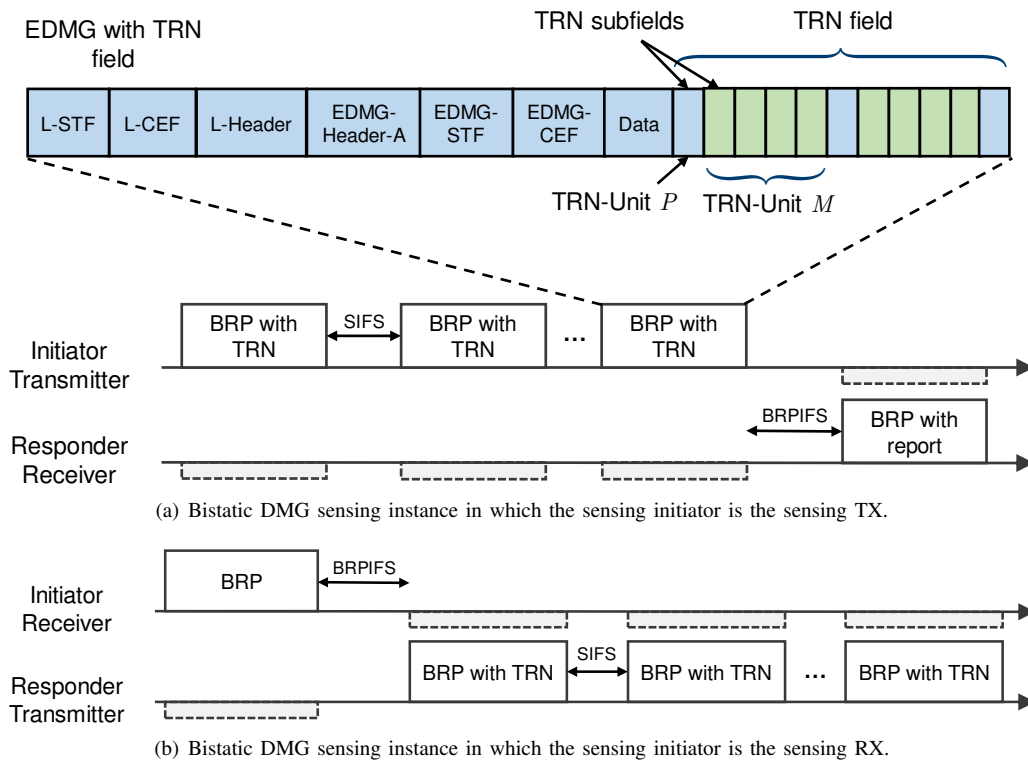


Fig. 14. Examples of DMG sensing instance for bistatic sensing.

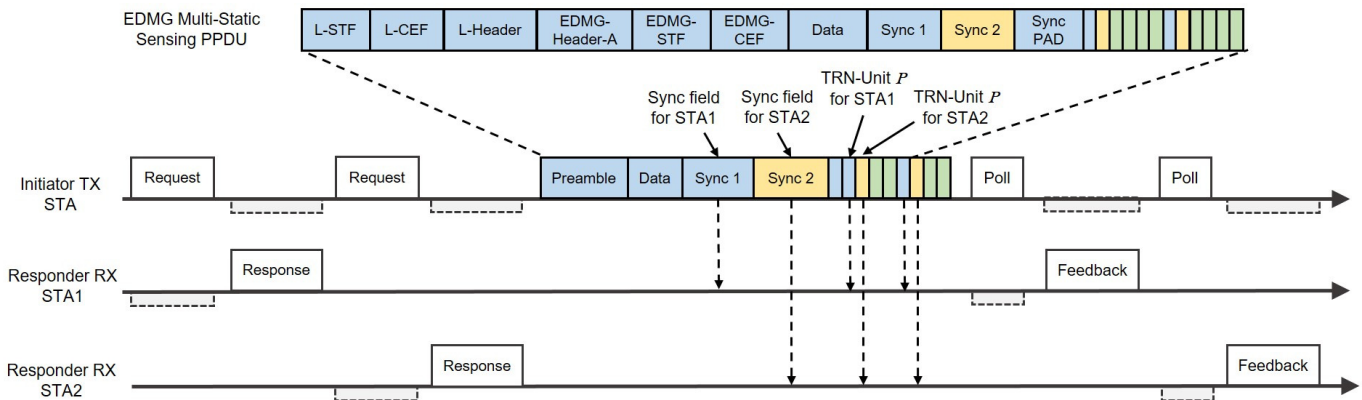


Fig. 15. Example of EDMG multistatic sensing instance.

Unlike coordinated monostatic sensing, the sounding phases of the different responders are sequential in the sounding phase of coordinated bistatic sensing, where the sounding procedure for each responder is the same as that of bistatic sensing.

6) *Passive Sensing*: In passive sensing, transmissions that are not specifically designed for sensing are used by other devices for sensing, such as beacon frames, sector sweep (SSW) frames, and short SSW frames. IEEE 802.11bf has provided an efficient downlink DMG passive sensing method based on the beacon frames in the beacon transmission interval (BTI) of a beacon interval (BI). Note that in (E)DMG, beacons are periodically transmitted in BTI to many directions (sectors) for network announcements and initiator transmit sector sweep (I-TXSS) at the AP. Support for passive sensing in the beacon is optional and is indicated by the Passive Sensing Support

subfield that is set to 1 in the Short Sensing Capability element transmitted in the beacon frames. During the transmission of the beacon frames, non-AP STAs can find the sector ID of a beacon that provides the highest signal quality. In IEEE 802.11ay, non-AP STAs do not need to know the specific transmit direction (sector) corresponding to the sector ID of a beacon with the highest signal quality, but only need to feed it back to the AP. However, in the passive sensing of IEEE 802.11bf, STAs that are interested in sensing need to know in which direction the beacon was transmitted and the location information of the AP to interpret the obtained sensing. To this end, STAs request sensing information by sending an Information Request frame to the AP, while the AP responds with an Information Response frame that contains the beacon directions and the AP location.

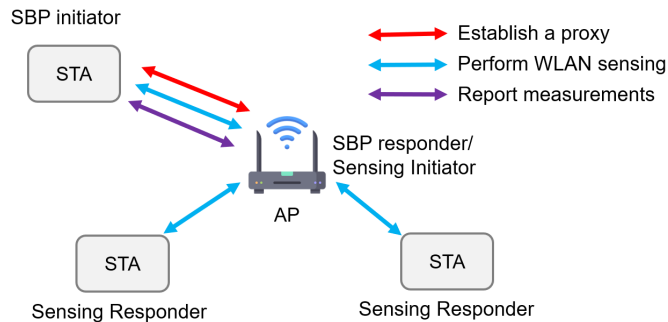


Fig. 16. Illustration of sensing by proxy.

An uplink DMG passive sensing method based on association beamforming training (A-BFT) of BI is also proposed in [71]. This differs from BTI, in that it enables an AP to perform I-TXSS, A-BFT following the BTI performs responder transmit sector sweep (R-TXSS) at the STAs by using SSW frames or Short SSW frames. Based on this, A-BFT can be used by an AP for passive sensing. Similar to the procedure of the beacon based passive sensing method for downlink, an AP that wants to sense the environment uses the received SSW frames or Short SSW frames to perform passive sensing. To obtain sensing information about the direction of each sector of SSW/Short SSW frames and the STA location, the AP sends an Information Request frame to the non-AP STA, and the non-AP STA returns the required information by using the Information Response frame. Note that the AP can obtain passive sensing results from multiple non-AP STAs to provide a broader sensing area.

D. Sensing by Proxy Procedure

The sensing by proxy (SBP) procedure allows a non-AP STA (SBP initiator) to request an AP (SBP responder) to perform WLAN sensing on its behalf, as shown in Fig. 16. In particular, the SBP initiator STA may obtain sensing measurements of the channel between an AP and one or more non-AP STAs in the SBP. To establish an SBP procedure, the SBP initiator shall first send an SBP Request frame to an SBP capable AP as a proxy. After accepting the SBP procedure request, the AP performs a WLAN sensing procedure with one or more non-AP STAs. In this stage, the STA as SBP initiator can participate as a sensing responder in this WLAN sensing procedure to enlarge the sensing area. Finally, the AP reports the obtained sensing measurements back to the SBP initiator that requested them. With the execution of the SBP procedure, it is possible for a non-AP STA to obtain necessary sensing measurements for detecting and tracking changes in the environment.

E. Presence Detection under IEEE 802.11bf sub-7GHz Sensing

To show how IEEE 802.11bf works for a certain sensing application, we take presence detection as a specific example. Suppose that the presence detection task is initiated at AP, and the TB sensing measurement in 802.11bf is used. In this case,

AP as the sensing initiator chooses a few sensing capable STAs in the home, such as smart TV, as the sensing responders to set up a sensing procedure. To increase the sensing coverage, AP can repeat the long training field (LTF) a few times to increase the SNR. AP can also choose to involve more sensing responders at different locations to increase the sensing coverage and transmit/receive diversities. AP could perform downlink sensing with NDPA sounding phase and/or perform uplink sensing with TF sounding phase. If NDPA sounding phase is used, CSI is estimated at the STAs and reported to AP. AP could first use a long sensing period to detect if there are moving targets in the home by estimating the stability of CSI. Then AP could further decrease the sensing period to capture more information on the moving target and recognize the target through its Doppler information (e.g., through the micro-Doppler signature). If the target becomes static, breath/heart beat detection based on CSI or other approaches could be adopted to detect the target⁹. The detection results are then reported to the upper layer to enable various applications. The sensing procedure solicited by the present detection task can be terminated if it is no longer needed.

F. Similarities and Differences between Sub-7GHz Sensing and DMG Sensing

Although we have elaborated on the sensing procedure for both sub-7GHz sensing and DMG sensing by discussing their shared terminologies and features, it is worth further pointing out their similarities and differences from the perspectives of both PHY and MAC layers, and accordingly identifying their encountered challenges, the resultant sensing performance, and their corresponding usage scenarios.

First, sub-7GHz and DMG sensing share the same technical challenges to be tackled. The first challenge is the estimation errors of CSI. In cases of separated transmission and reception in Wi-Fi devices, various deviations (such as carrier frequency offset and symbol timing offset) remain in the CSI during channel estimation, affecting the performance of CSI-based sensing. To address the synchronization issues caused by separation, different approaches have been introduced in the sub-7GHz and DMG sensing standards. For instance, DMG antennas exhibit strong directionality, thus allowing for better transmission and reception isolation. Therefore, by exploiting this, IEEE 802.11bf implements full-duplex (FD) operation in DMG sensing to mitigate the synchronization issues. On the contrary, since sub-7GHz does not currently incorporate FD, CSI correction for sub-7GHz relies solely on algorithms design. The second challenge is the requirement to enhance CSI stability. The CSI needed for Wi-Fi sensing is the CSI between the transmit and receive antennas, which is referred to as physical CSI. However, in reality, the CSI estimated at the RX is a mixture including the effect of transmit RF, receive RF, and the physical CSI. Power gain adjustments at both the TX and RX sides influence the CSI. To tackle this issue, IEEE 802.11bf suggests maintaining stable transmission power during measurements and reporting adjustments in RX

⁹Notice that the specific stability detection and recognition algorithms based on CSI are out of the scope of IEEE 802.11bf.

gain to enhance CSI robustness for both sub-7GHz and DMG sensing.

Next, sub-7GHz and DMG sensing have different sensing performances, as detailed in the following aspects.

- They have different BW and thus distinct range resolutions. Sub-7GHz supports a maximum of 320 MHz continuous BW measurement, while DMG has a BW of 1.76 GHz per channel (and larger BW can be achieved by aggregating multiple channels).
- Different carrier frequencies lead to different speed resolutions under the same coherent integration time and the same Doppler resolution.
- Additionally, under the same speed, different carrier frequencies result in different Doppler shifts, leading to different Pulse Repetition Frequencies (PRF) for Nyquist sampling.
- Different antenna apertures in the two frequency bands result in different spatial resolutions. In particular, sub-7GHz sensing supports up to 8 antennas/streams, while DMG sensing typically uses directional antennas.

In addition, sub-7GHz and DMG sensing have different usage scenarios. Specifically, sub-7GHz is suitable for applications requiring larger coverage, larger targets, and significant movements such as presence detection and activity recognition, while DMG is suitable for applications with smaller coverage areas, smaller targets, and fine movements such as heart rate monitoring and gesture control.

Summary and Lessons Learned: In this section, we first specify the possible role each STA could play, including sensing initiator/responder and sensing TX/RX, based on which different sensing configurations for IEEE 802.11bf are illustrated. We then proceed to introduce sub-7GHz sensing and DMG sensing sequentially with concrete examples provided to show their working mechanism. In particular, we elaborate four sessions in a typical sub-7GHz sensing procedure, including sensing capabilities exchange, sensing measurement session, sensing measurement exchange, and sensing measurement session termination. Among them, sensing measurement exchange could be further separated into two categories: TB and non-TB. For DMG sensing, we first discuss how DMG sensing is evolved from previous standards and its support for highly directional sensing, which is significantly different from sub-7GHz sensing. Different sessions of DMG sensing are then discussed, which is similar to that in sub-7GHz sensing. Among them, depending on the number and roles of the devices involved in sensing, DMG sensing measurement exchange could be classified into several types including monostatic, bistatic, multistatic, monostatic with coordination, bistatic with coordination, and passive, which are all discussed in detail. After that, we discuss SBP, which is a common feature in WLAN sensing and provide a concrete example about how presence detection task is implemented under 802.11bf sub-7GHz sensing. Finally, we further discuss the similarities and differences between sub-7GHz sensing and DMG sensing, which can be viewed as the lessons learned and thus are briefly reviewed below.

- Both sub-7GHz and DMG sensing encounter the issue of

CSI estimation errors due to imperfect synchronization and as a remedy, sub-7GHz mainly relies on algorithms design while DMS sensing implements FD operation.

- Both of sub-7GHz and DMG sensing face the challenge of maintaining CSI stability. To tackle this issue, maintaining stable transmission power during measurements and reporting adjustments in RX gain are proposed.
- Sub-7GHz and DMG sensing have different sensing performances in terms of BW, range resolution, speed resolution, PRF, and spatial resolution.
- The application scenarios for sub-7GHz and DMG sensing are different in the sense that sub-7GHz is suitable for macro-sensing applications while DMG sensing fits micro-sensing applications better.

V. IEEE 802.11BF: CANDIDATE TECHNICAL FEATURES

To enable and enhance sensing functionality, a variety of candidate technical features have been proposed by numerous industrial and academic experts during IEEE 802.11bf meetings. In the following, we focus on technologies that attracted the most attention.

A. Waveform and Sequence Design

The existing preamble waveform/sequences (e.g., Sync sequences) were specifically designed for communication systems, focusing on enhancing the communication performance, e.g., Peak-to-Average Power Ratio (PAPR). However, the properties of sensing (e.g., angle/range resolution, Doppler frequency) were not considered. In other words, new waveform/sequence and waveform evaluation metrics are needed in WLAN sensing.

In order to take sensing performance into account, one of the most straightforward ideas is to use the ambiguity function (AF) to evaluate the transmit waveforms [72]. The ambiguity function is one of the most widely used tools in radar waveform analysis, which processes the received signal through a matched filter and shows a R-D (Range-Doppler) map result. It is defined as [73]:

$$|\mathcal{X}_{a,b}(\tau, f_d)| = \left| \int_{-\infty}^{\infty} S_a(t) S_b^*(t - \tau) e^{j2\pi f_d t} dt \right|^2, \quad (1)$$

where $S_a(t)$ and $S_b(t)$ denote two sequences to be matched, and τ and f_d denote time delay (range) and Doppler frequency, respectively. $|\mathcal{X}_{a,b}(\tau, f_d)|$ is called the auto ambiguity function (AAF) if $S_a(t) = S_b(t)$, and the cross ambiguity function (CAF) if $S_a(t) \neq S_b(t)$. A demo of magnitudes of the AAF and CAF outputs is shown in Fig. 17(a)(d), using a BW setup of 20 MHz and sequences

$$CE0 = [Ga^7, -Gb^7, Ga^7, -Gb^7, Ga^7, Gb^7, Ga^7, Gb^7], \quad (2)$$

$$CE1 = [Ga^8, -Gb^8, Ga^8, -Gb^8, Ga^8, Gb^8, Ga^8, Gb^8] \quad (3)$$

with 128-length Golay sequences Ga^7, Gb^8 , as defined in IEEE 802.11ay [74].

A good AAF should look like a “thumbtack” shape that has a peak at the origin and low/zero side lobes elsewhere, while a good CAF should have as small as possible magnitudes

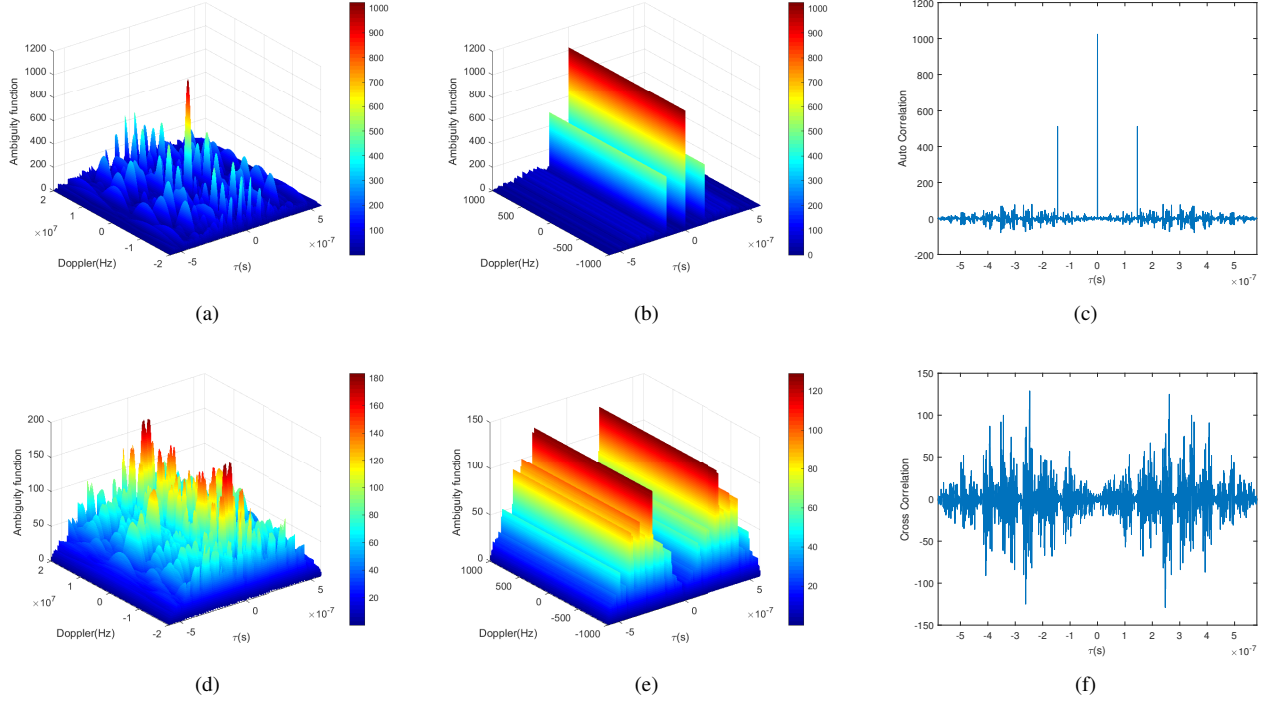


Fig. 17. A demo AAF for CE0 in the range of (a) $[-20\text{MHz}, 20\text{MHz}]$, (b) $[-1000\text{Hz}, 1000\text{Hz}]$; (c) Auto Correlation result. A demo CAF for CE0 and CE1 in the range of (d) $[-20\text{MHz}, 20\text{MHz}]$, (e) $[-1000\text{Hz}, 1000\text{Hz}]$; (f) Cross Correlation result.

$-M(r,7) \times G^p$	$M(r,7) \times G^p$	$M(r,0) \times G^p$	$M(r,1) \times G^p$	$M(r,2) \times G^p$	$M(r,3) \times G^p$	$M(r,4) \times G^p$	$M(r,5) \times G^p$	$M(r,6) \times G^p$	$M(r,7) \times G^p$	$M(r,0) \times G^p$							
----------------------	----------------------	----------------------	----------------------	----------------------	----------------------	----------------------	----------------------	---------------------	---------------------	---------------------	---------------------	---------------------	---------------------	---------------------	---------------------	---------------------	---------------------

Fig. 18. Sync subfield structure.

	1	2	3	4	5	6	7	8
1	0	0	0	0	60	80	52	72
2	0	0	0	0	80	52	76	60
3	0	0	0	0	60	80	52	72
4	0	0	0	0	80	52	76	60
5	60	80	60	80	0	0	0	0
6	80	52	80	52	0	0	0	0
7	52	76	52	76	0	0	0	0
8	72	60	72	60	0	0	0	0

Fig. 19. Correlation of 8 sequences.

everywhere. These two properties will make the design more robust to timing offset and frequency offset, and help resolve the target parameters more accurately after matched filtering [75]. It can be clearly observed that AAF and CAF usually do not have a good performance at the whole BW, as shown in Fig. 17(a)(d). However, considering the Doppler frequency in actual scenarios (e.g., a living room), it is much lower than the signal BW, meaning that an AF design can be narrowed down to a much smaller area around the origin. Driven by this, a new concept named LAZ/ZAZ (Low/Zero Ambiguity

Zone), and its corresponding signal designs are presented in [76], where LAZ/ZAZ can be considered as a local AF limited by a maximum Doppler frequency and maximum time delay. Fig. 17(b)(e) shows an example for local AF with maximum Doppler frequency $f_{max} = f_c * v_{max}/c = \frac{60\text{GHz} * 5\text{m/s}}{3 * 10^8\text{m/s}} = 1000\text{Hz}$. It is observed that the local AF has good “ambiguity” as the maximum value of the AAF side lobes and maximum value of CAF are relatively very low in the region of interest.

In the case of DMG sensing, the auto/cross correlation also serves as a surrogate function for local AAF/CAF. Looking back at Fig. 17(b)(e), any magnitudes of AF along Doppler frequency axis with fixed time delay remain constant, which means that the evaluation of local AF performance can be restricted to a certain Doppler frequency. The auto/cross correlation in Fig. 17(c)(f) is actually the cross section of the local AAF/CAF at zero Doppler frequency. As such, IEEE 802.11bf currently uses auto/cross correlation to evaluate waveform designs.

By considering the auto/cross correlation performance of the sequences, a new structure of synchronization sequences for Sync subfields in multi-static sensing is proposed [77], as shown in Fig. 18, where r denotes the index of the STA. The Sync subfields of different STAs use different rows of the

coefficient matrix $M(r, c)$, which is defined as

$$M = \begin{bmatrix} 1 & -1 & 1 & -1 & 1 & 1 & 1 & 1 \\ 1 & -1 & 1 & -1 & 1 & 1 & 1 & 1 \\ 1 & 1 & -1 & -1 & 1 & -1 & -1 & 1 \\ 1 & 1 & -1 & -1 & 1 & -1 & -1 & 1 \\ -1 & 1 & -1 & 1 & 1 & 1 & 1 & 1 \\ -1 & 1 & -1 & 1 & 1 & 1 & 1 & 1 \\ 1 & -1 & -1 & 1 & -1 & -1 & 1 & 1 \\ 1 & -1 & -1 & 1 & -1 & -1 & 1 & 1 \end{bmatrix}. \quad (4)$$

Therefore, the proposed design can support a maximum of 8 different STAs for sensing simultaneously. For r from 1 to 8, G_i^p is $Ga^7, Ga^8, Ga^7, Ga^8, Gb^7, Gb^8, Gb^7, Gb^8$, and G_j^p is $Gb^7, Gb^8, Gb^7, Gb^8, Ga^7, Ga^8, Ga^7, Ga^8$, respectively. The Sync subfields need to be designed to have high auto correlations and low cross correlations. Fig. 19 gives the performance measurement of the synchronization subfield proposed in [77], where the elements on the diagonal denote the maximum of the sidelobe of the auto correlation of the same Sync sequence and the non-diagonal elements denote the maximum magnitude of the cross-correlation of different Sync sequences. Notice that the maximum value of the auto correlation for Syn sequences is 1024. It is shown that the proposed Sync sequences can ensure that the cross-correlation between the initial or last 4 sequences is 0, while the cross-correlation between the initial 4 and last 4 sequences is kept at a low level.

B. Feedback Types

In order to implement various sensing services efficiently, it is critical to provide appropriate and accurate measurement results in the feedback. To support this, one or more types of sensing measurement results and their formats need to be defined depending on the requirements of different sensing applications at sub-7GHz and 60 GHz.

1) *Sub-7GHz Sensing*: for sub-7GHz sensing, the potential feedback types include the full CSI matrix, partial CSI [78], truncated power delay profile (TPDP)/truncated channel impulse response (TCIR) [79], and frequency-domain differential quantization [80], etc. First, it is fairly straightforward to take advantage of measurements that are already defined in the IEEE 802.11 standard, such as those for explicit feedback¹⁰. Thus, the full CSI matrix, a typical measurement/feedback type that has been extensively used in various sensing implementations, is repurposed for IEEE 802.11bf in the sub-7GHz band. It captures the wireless characteristics of the signal propagation between the TX and the RX at certain carrier frequencies, and thus represents the channel frequency response (CFR). Because CSI is a direct result of the channel estimation, it retains the full environmental information and has no information loss compared to other feedback types. Next, by noting that some sensing applications use only either the amplitude or the phase of the CSI, not both, it is proposed to reduce the overhead by feeding back either the

amplitude or the phase [78]. Another alternative feedback type is TPDP/TCIR. Specifically, [79] proposed the TPDP/TCIR as a potential sensing measurement result in explicit feedback, as shown in Fig. 20(a). By performing an inverse fast Fourier transform (IFFT) on the CSI in the frequency domain, the channel impulse response (CIR) in the time domain can be calculated. It describes the multipath propagation delay versus the received signal power for each channel. Since the maximum range of sensing is a few dozen meters [60], the first few complex values of the CIR already contain the desired environment information and thus can be reported as sensing measurement results. Furthermore, to further reduce the feedback overhead in the frequency domain, a frequency-domain differential quantization was proposed in [80], as shown in Fig. 20(b). The main idea behind this is to report the differential signal obtained by subtracting the quantized signal of the previous subcarrier from the signal of the current subcarrier. Since the quantization range is reduced by the differential operation, the feedback overhead is reduced while ensuring the integrity of the measurement information.

2) *DMG Sensing*: as for the 60 GHz band in DMG sensing, three types of sensing measurement result have been identified for IEEE 802.11bf, i.e., channel measurement for IEEE 802.11ad/ay, Range-Doppler-Angular map (R-D-A map) and target-related parameters. First, similar to TCIR, the channel measurement in IEEE 802.11ad/ay returns the CIR corresponding to each TRN subfield, where the number of returned delay taps is optional. Next, an R-D-A map, also known as sensing image in IEEE 802.11bf, provides an “image” of the surrounding environment, which can be up to a four-dimensional (4D) image data consisting of range, Doppler, azimuth, and elevation. Note that by combining some or all of the data from the four dimensions, the sensing image can be a 2D, 3D, or up to 4D image. By detecting the area of higher energy on the R-D-A map, it is possible to know in which location there is a reflector or target, and based on this information, subsequent sensing implementation can thus be performed. Furthermore, since direct reporting of R-D-A maps is inefficient and has a high feedback overhead, it is most effective to report target-related parameters, such as the position and Doppler of the target, directly after target detection processing of the R-D-A maps. A typical sensing image processing flow diagram [81] for 60 GHz is shown in Fig. 21, from which all three types of sensing measurement results can be obtained.

C. Quantization and Compression

The measurement results need to be quantified before they can be reported to the sensing initiator to reduce the feedback overhead. However, the quantization of measurement results introduces inevitable quantization errors. As a result, designing an efficient and accurate quantization and compression method is critical for WLAN sensing.

The potential quantization and compression methods for IEEE 802.11bf include the legacy quantization procedure in IEEE 802.11n [82], the simplified scaling and quantization method [83], the power-of-two scaling and quantization

¹⁰Note that the explicit feedback corresponds to the case when the RX needs to directly send the downlink measurements to the TX, while the implicit feedback corresponds to that the TX uses channel reciprocity to obtain the downlink measurements based on the uplink measurements.

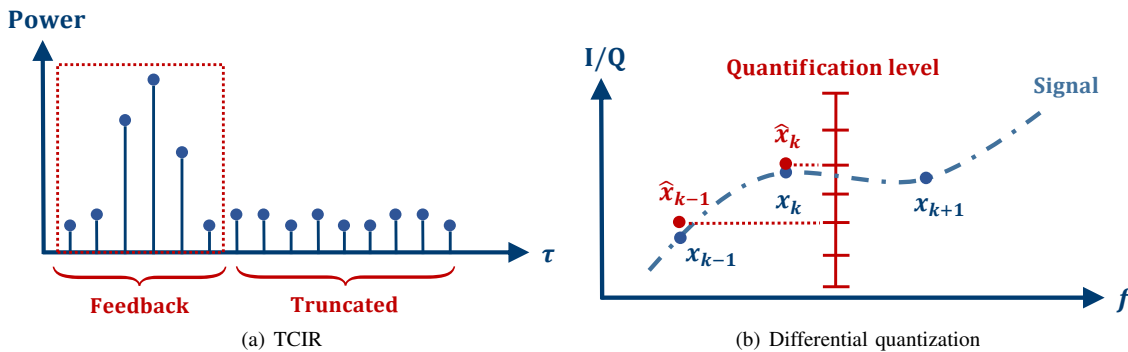


Fig. 20. Potential feedback types for sub-7GHz.

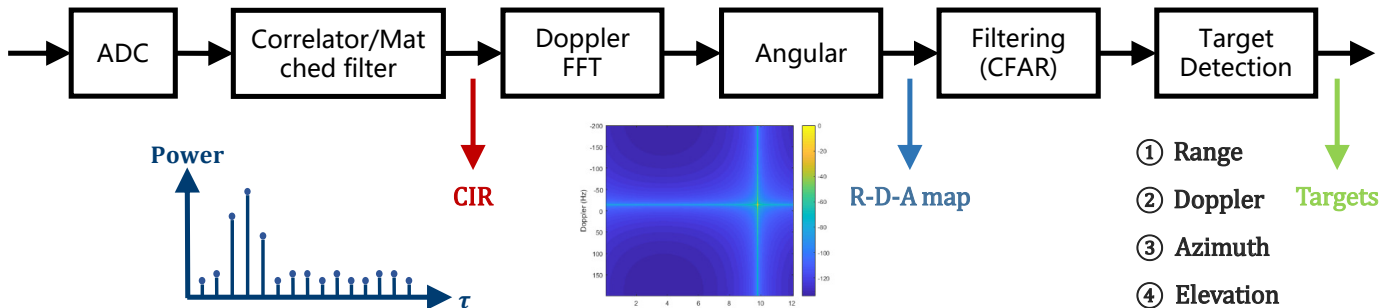


Fig. 21. A typical sensing image processing flow diagram [81] for 60 GHz. Here, ADC stands for Analog-to-Digital converter and CFAR stands for Constant False Alarm Rate.

method [84], and the fractional scaling and quantization method [85]. First, as a proven method, the CSI matrix quantization procedure in IEEE 802.11n [82] (or with minor modifications) can be reused for sensing services in IEEE 802.11bf, which is reviewed briefly in the following. Denote $m_H(k)$ as the maximum of the In-phase and Quadrature components of each element of the CSI matrix $\mathbf{H}(k)$ in each subcarrier k . Prior to quantization, a scaling factor of the CSI matrix needs to be calculated to improve the dynamic range of quantization. The scaling factor $M_H(k)$ in IEEE 802.11n is obtained by quantizing $m_H(k)$ to three bits in the decibel (dB) domain and then converting back to the linear domain. As a result, the In-phase and Quadrature components of each element in $\mathbf{H}(k)$ are scaled and quantized to N_b bits as

$$h^q(k) = \text{Round} \left(\frac{h(k)}{M_H(k)} \left(2^{(N_b-1)} - 1 \right) \right), \forall k, \quad (5)$$

where $h(k)$ denotes the In-phase/Quadrature components of each element of the CSI matrix $\mathbf{H}(k)$, $h^q(k)$ denotes the corresponding quantized data, N_b denotes the number of bits of quantized data, and $\text{Round}(\cdot)$ rounds a number to its nearest integer. However, the procedure of the CSI matrix quantization in IEEE 802.11n requires considerable computational complexity due to the need for repeated linear to dB and dB to linear conversions. In addition, multiplication and division operations need to be performed prior to quantization.

To avoid these drawbacks, [83] uses a uniform linear scaling factor M_H^{lin} for all subcarriers and simplifies the transformation of M_H from $m_H(k)$ by directly setting M_H^{lin} to the maximum value in $m_H(k)$, $\forall k$, i.e., $M_H^{lin} = \max_k m_H(k)$. The

corresponding quantized In-phase and Quadrature components can be obtained by simply replacing $M_H(k)$ in (5) as M_H^{lin} .

Furthermore, [84] proposed a low-complexity scaling and quantization method by using the power-of-two scaling factor for the CSI matrix. Let N_p denote the number of bits of original data. To maximize the dynamic range of quantization, the power-of-two scaling factor α_H is chosen to ensure that $2^{(N_p-2)} \leq \alpha_H m_H(k) \leq 2^{(N_p-1)} - 1$. The final quantized In-phase and Quadrature components of each element in $\mathbf{H}(k)$ are given by

$$h^q(k) = \text{Round} \left(\alpha_H h(k) \left(2^{(N_b-N_p)} \right) \right), \forall k. \quad (6)$$

Note that since $h(k)$ only needs to be multiplied and divided with powers of two, a binary shift operation can be performed in hardware or software to greatly reduce the computational complexity. Nevertheless, compared to the real-value scaling as in IEEE 802.11n, both the simplified scaling and the power-of-two scaling lead to a relative increase in the quantization error due to the reduction in the dynamic range of quantization.

In addition, considering the trade-off between computational complexity and quantification accuracy, a fractional scaling and quantization method is proposed in [85]. Notice that the scaling factor in (5) can be considered as the ratio between two numbers (α and β) as

$$\text{Round} \left(\frac{2^{(N_b-1)} - 1}{m_H(k)} h(k) \right) = \text{Round} \left(\frac{\alpha}{\beta} h(k) \right), \quad (7)$$

where β can be constrained to be a power of two to reduce the computational complexity and α can be chosen among a set of pre-defined values to optimize the scaling factor. In order

to obtain the best performance, the maximum of α/β should be found while ensuring the following inequality:

$$\frac{\alpha}{\beta} \leq \frac{2^{(N_b-1)} - 1}{m_H(k)}. \quad (8)$$

By expanding the size of the set of α , the performance of fractional scaling can approach that of real-value scaling specified in IEEE 802.11n.

Summary and Lessons Learned: In this section, we discuss candidate technical features that have attracted the most attention during IEEE 802.11bf meeting including waveform and sequence design, feedback types, and quantization and compression method. Specifically, we first introduce AAF and CAF, which serve as the metric and tool to evaluate waveform design, based on which new structures of synchronization sequences are proposed for enhanced sensing performance. Then, we discuss potential feedback types for sub-7GHz sensing including full CSI matrix, partial CSI, TPDP/TCIR, and frequency-domain differential quantization. For DMG sensing, three general feedback types including CIR, R-D-A map, and target-related parameters are elaborated. Finally, we address quantization and compression of measurement feedback, in which both previously proven methods specified in IEEE 802.11n and newly proposed methods including uniform linear scaling and quantization, low-complexity power-of-two scaling and quantization, and fractional scaling and quantization are adequately illustrated. It is worth pointing out that these technical features have not been frozen yet and subsequent research and new proposals will have significant impact on their finalization in this amendment.

VI. SIMULATION AND CHANNEL MODEL

In order to evaluate different proposals, simulation and channel models have been discussed in IEEE 802.11bf. Accordingly, the evaluation methodology [86] and channel model document [87] have been developed to facilitate the development of the draft amendment.

A. Evaluation Methodology

To more objectively and effectively promote the standardization process in IEEE 802.11bf, different technical proposals can be evaluated according to the evaluation methodology document [86], in which PHY performance, a limited set of simulation scenarios, and parameters that might be used when evaluating the performance of different contributions are summarized.

As yet, two indoor scenarios with dense multi-paths have been proposed (i.e., an indoor living room and conference room) for the simulation, where the room size and the properties of various environmental objects are all strictly defined by the IEEE 802.11bf. During the simulation, one TX-RX pair and a moving target are assumed, and two types of antennas (directional and isotropic) can be adopted. In particular, the TX and RX communicate with each other in a single-input single-output (SISO) mode since the desired antenna pattern can be added to the isotropic antenna. Moreover, in order to simulate the above scenarios, traffic models and hardware impairments

are required. As specified in [88], they can be the same as that of IEEE 802.11ax for sub-7GHz [89] and IEEE 802.11ay for 60 GHz [90].

Furthermore, evaluation criteria between the different contributions need to be defined for IEEE 802.11bf in order to assess the merits of each contribution. As opposed to previous IEEE 802.11 task groups that focused on the communication criteria, i.e., throughput and packet error rate (PER), the IEEE 802.11bf task group adopted estimated parameters accuracy as a metric to evaluate the PHY performance of WLAN sensing. In general, for parameter estimation, the accuracy describes how close the estimated parameter of the intended target (e.g., range, velocity, angle, etc.) are to the ground truth¹¹, and it is described by the root mean square error (RMSE) of the parameters to be estimated, as defined below:

$$\text{RMSE} = \sqrt{\frac{1}{N} \sum_{n=1}^N (\hat{x}_n - x_n)^2} \quad (9)$$

where \hat{x}_n is the estimated parameter, x_n is the ground truth, and N is the number of observations. According to [86], two comparison criteria of the PHY performance based on the accuracy of estimated parameters are: an *accuracy vs. SNR curve* and a *histogram of accuracy*. These are adopted for different operation modes in different scenarios. The accuracy vs. SNR curve indicates the WLAN sensing estimation accuracy with different SNRs. Usually, accuracy improves as SNR increases. As for the histogram of accuracy, the SNRs caused by a moving target on a certain predefined trajectory are different during the WLAN sensing simulation, which results in different estimation accuracies. Based on the estimated accuracy information (e.g., range, velocity, and angle) for each sample, a histogram of accuracy during the simulation can be calculated.

B. Channel Model

The initial idea of channel modeling for a WLAN Sensing system was presented in [91], where some initial thinking about the goals and necessity of the new channel modeling for WLAN sensing were discussed. Compared with previous channel models operating at sub-7GHz (e.g., IEEE 802.11ax [92]) and 60 GHz (e.g., IEEE 802.11ay [93]) that focused only on the communication characteristics in specific frequency bands, the new channel model for WLAN sensing should mainly focus on providing accurate space-time characteristics of the propagation channel arising from the device and freely moving targets both in the sub-7GHz and 60 GHz bands. For this reason, two preliminary channel models aiming at WLAN Sensing were established in the channel model document [87], each of which is discussed briefly below.

The first proposed channel model (known as the ray-tracing-based channel model) is a deterministic model that uses a ray-tracing technique to process channel realization. Ray-tracing technique is a numerical computational electromagnetic method that uses computer program to provide

¹¹Ground truth is information provided by direct observation and measurement that is known to be true, rather than by inference.

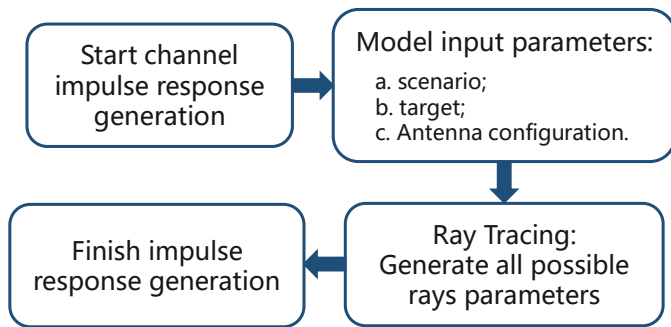


Fig. 22. Process of ray-tracing-based channel realization.

estimates for multipath parameters, e.g., path loss, angle of arrival/departure (AOA/AOD), and time delays, by assuming the transmitted signal as a particle [94]. As illustrated in Fig. 22, the ray-tracing-based channel model selects scenario, target, and antenna configurations as inputs, and then generates all possible time-variant rays for each TX-RX pair in different simulation frames. Given these, a time-variant CIR is generated. For example, in [87], two simulation schemes with different configurations in a living room scenario with a device and a freely moving target are presented, in which an AP (TX) and STA (RX) are in a monostatic setting and are equipped with a directional/isotropic antenna. The simulation results show the power delay profile (PDP) at different snapshots.

However, ray-tracing-based methods suffer from large computational complexity and can not represent the sensing uncertainty in real measurements such as the unpredictable motions of other objects, and random perturbations of scatter (e.g., diffracted and scattering rays), which are the unrelated rays to those of the target. In order to solve these drawbacks, the data-driven hybrid channel model (DDHC) was also proposed in [87], [95]. In this so-called hybrid channel model (see Fig. 23 as an example), rays between TX-RX pairs are divided into target-related rays and target-unrelated rays [95], [96], where the target-related rays are generated via the aforementioned ray-tracing tool and the target-unrelated rays are generated by adopting an autoregressive model of existing standardized channel models (IEEE 802.11ax for sub-7GHz [92] and IEEE 802.11ay for 60 GHz [93]). On the other hand, real datasets collected from the experiments serve to refine the parameter tuning by minimizing the Kullback-Leibler (KL) divergence between the real and simulated datasets [95], [96].

Fig. 24 shows spectrograms of human motion at both sub-7GHz and 60 GHz, where the conference room scenario with a monostatic transceiver is considered and a person is walking around the room. The comparison results indicate that the ray-tracing-based datasets differ from both the DDHC-based and the real-world datasets in that the motion patterns of the DDHC-based and real spectrogram images have peaks, while the ray-tracing-based ones are smoother. This is due to the unpredictable reflections from the wall and random scatter as well as the irregular movements of the sensing target in the real-world. Furthermore, it is verified that the sensing performance of the DDHC model is close to that of a real world dataset and significantly outperforms the performance

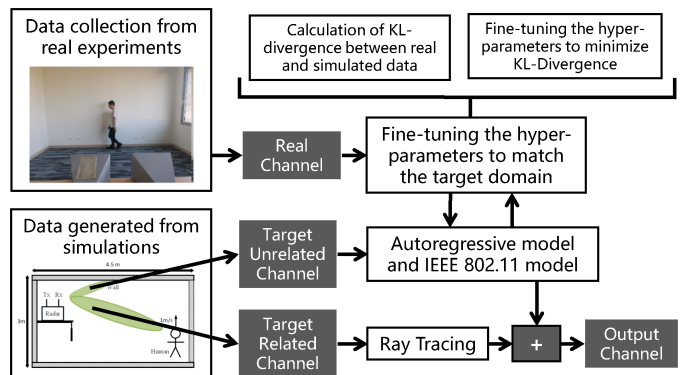


Fig. 23. Process of DDHC-based channel realization.

of the ray-tracing model [87].

C. Link-Level Simulation

Based on the authenticity and objectivity of the performance verification, IEEE 802.11bf task group pointed out that it is necessary to build an IEEE 802.11bf simulation platform to perform WLAN sensing simulations, and the corresponding link level simulation was proposed [97]. The system structure of the link-level simulation platform for WLAN sensing is shown in Fig. 25, and the specific flow of the simulation is illustrated.

It is clear that the WLAN sensing link-level simulation mainly contains a waveform generation module, transmitter module, environment/channel module, receiver module, and signal processing and performance evaluation module. Specifically, the waveform generation module is mainly responsible for the generation of different waveforms, which consists of new sequences, new waveforms, normal WLAN PPDU, and modified WLAN PDUs, etc. The TX/RX module focuses on the transmission/reception of the signal based on some array information, including array geometry, element radiation pattern, and location, etc. Then, the environment/channel module needs to generate the channel matrices according to the transceiver antenna configurations and the parameters of the targets and multi-path defined in [86]. Finally, in the signal processing and performance evaluation module, the received signals are processed with different algorithms in order to estimate the parameters of the targets and analyze their relevant performance metrics. With the link-level simulation, the sensing accuracy performance can be calculated based on the estimated parameters and ground truth used for the simulation. An example of the link-level simulation with a ray tracing channel at 60 GHz in an indoor scenario is shown and discussed in [98], which verifies that WLAN sensing simulation can be conducted based on this link-level simulation platform.

Summary and Lessons Learned: In this section, we discuss the simulation and channel models for evaluating different proposals. We start from evaluation methodology by introducing two indoor scenarios for evaluation and their corresponding setup. Then we introduce RMSE as a performance metric for WLAN sensing, which leads to two higher level comparison

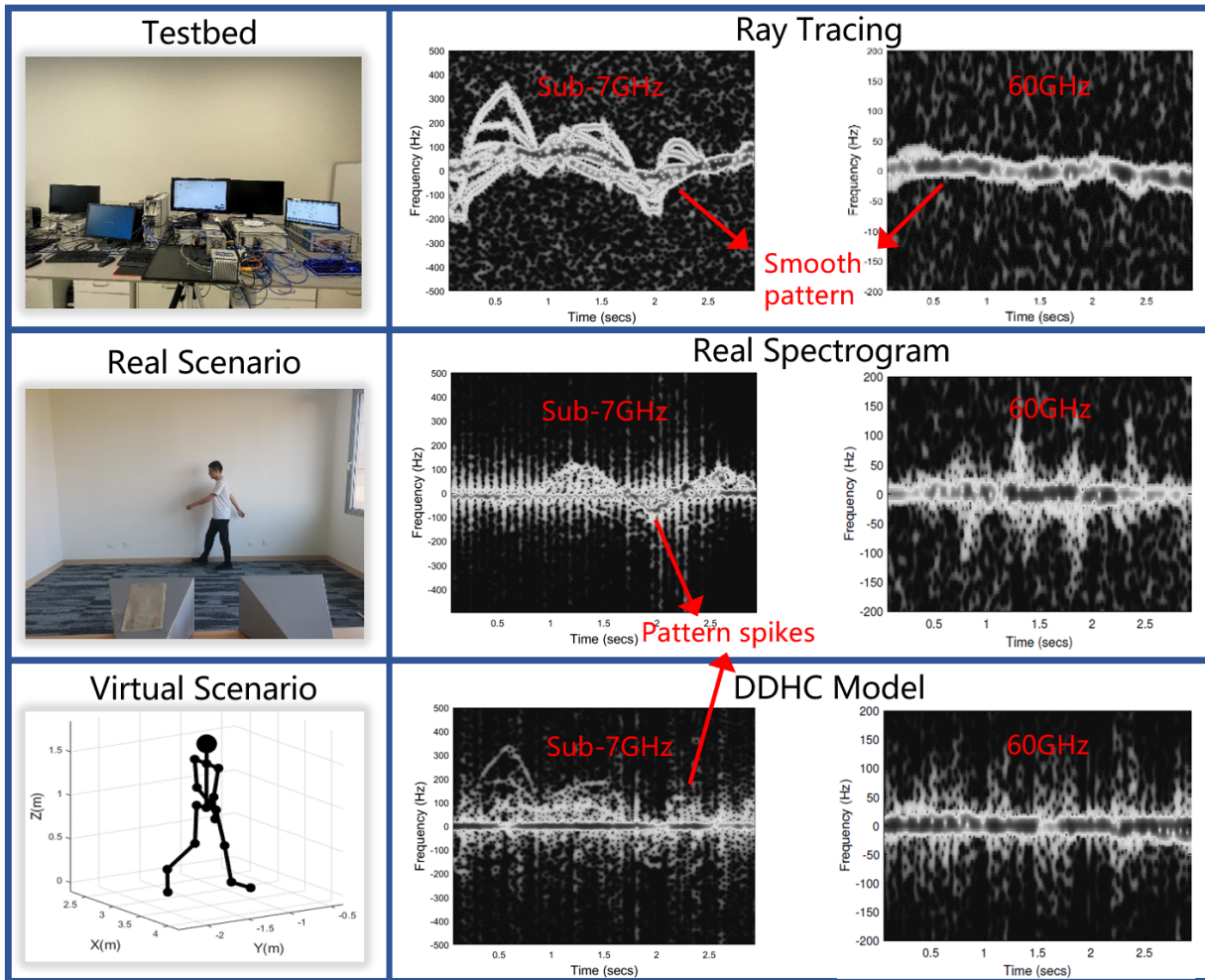


Fig. 24. Spectrograms of human motion at sub-7GHz and 60 GHz.

criteria: Accuracy vs. SNR curve and Histogram of accuracy. Next, two channel modeling approaches including ray-tracing and DDHC are elaborated in detail, followed by a concrete example with comparison between these two modeling methods in both sub-7GHz and 60 GHz. Finally, we discuss the link-level simulation platform composed of five modules, and outline its framework. The lessons learned in this section can be split into three portions:

- In terms of evaluation methodology, RMSE is regarded as the metric to characterize the PHY performance of WLAN sensing. Based on RMSE, two high level metrics: Accuracy vs. SNR curve and histogram of accuracy can be adopted for evaluation in different scenarios such as static versus moving targets estimation.
- In terms of channel modeling approach, conventional ray-tracing techniques suffer from high computational complexity and inability to capture sensing uncertainty in real measurements such as the unpredictable motions of moving objects. The newly proposed DDHC, enhanced by data-driven approaches, is observed to yield better modeling performance.
- Link-level simulation is crucial for sensing performance evaluation, in which new waveform design, TX/RX adap-

tation and configuration, channel modeling, and sensing algorithms could be jointly validated.

VII. FUTURE RESEARCH DIRECTIONS

During the development of 802.11bf amendment, most of the standard related problems have been resolved by 11bf TG. However, there are a few technical problems and challenges that need to be further addressed and explored to improve the sensing performance and facilitate promising ubiquitous sensing applications in a secure, sustainable, and compatible manner under the IEEE 802.11bf standards.

A. Multi-Link Sensing

Sensing in 802.11bf mainly focused on the scenario with a single radio link between peer stations. With the commercialization of Wi-Fi 7 in a few years, a large number of multi-link devices will appear in the market. Multi-link is one of the key techniques that could be utilized to improve the sensing performance, and the coordination of different links can help better support various new sensing applications. For example, to ensure the sensing performance for fast moving targets (such as moving vehicles), the sounding repetition frequencies

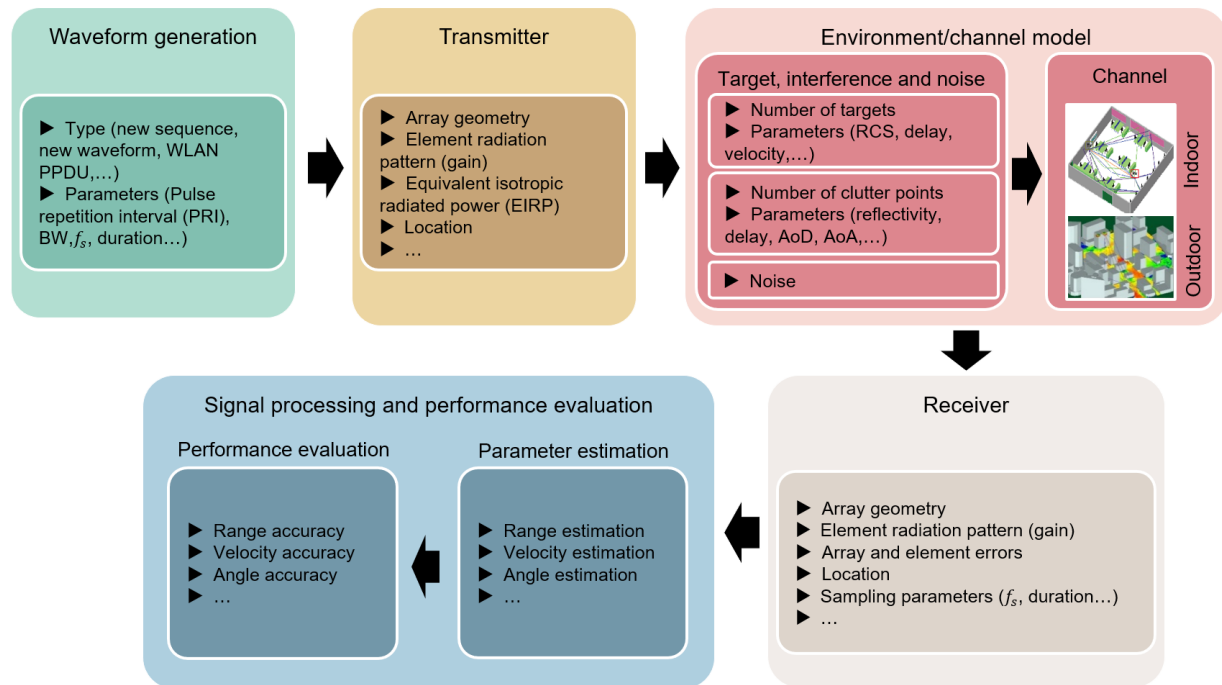


Fig. 25. Framework of link level simulation platform.

need to be high enough to achieve the Nyquist sampling. A multi-link sensing capable device could realize this by setting separated sensing link(s) and reporting link(s) to reduce the occupation of report in the sensing link.

Besides, a multi-link sensing capable device is able to perform sensing at multiple operating frequencies (e.g., 2.4/5/6 GHz) and provide sensing measurement at different frequencies. Generally, to fully utilize the sensing measurement up-clocked results at different frequencies, further investigations are needed mainly on two different cases. In the first case, if the sensing measurement results from multiple frequencies are processed non-coherently or separately, then the fusion scheme for combining the separately processed sensing results is key to fully utilize the frequency diversities and thus deserves further investigation. In the second case, if the sensing measurement results from multiple frequencies are processed coherently as a frequency sparse estimation problem, the research on their joint signal processing are needed. The characterization of the fundamental limit of sensing performance (e.g., estimation) and the corresponding high-performance algorithms under the constraints of real Wi-Fi systems are both promising research directions.

Another potential research direction is the compression scheme of the multi-band sensing measurement results. In 802.11bf, CSI matrix without any compression is adopted as the only sensing measurement feedback type. However, the feedback overhead of CSI matrix increases when the sensing BW increases, and such overhead may further increase if the sensing is conducted over multiple frequency bands. To reduce the feedback overhead, joint compression scheme of the CSI matrices over multiple bands should be further analyzed.

Furthermore, mmWave is under discussion as a potential

technique for Wi-Fi 8 [99]–[101] to meet the high throughput and low latency requirements of future Wi-Fi systems. Different from the DMG/EDMG that also operate at mmWave, the potential new mmWave standard may consider using an up-clocked version of sub-7GHz PHY to simplify the baseband processing. Once this new mmWave standard is adopted in Wi-Fi 8, new problems will be introduced, and more research activities may be needed to resolve them. The electromagnetic properties of the mmWave are quite different from that in sub-7GHz and the spacing between different frequencies is further enlarged. These issues may bring new technical issues for CSI matrices compression and signal processing.

B. Sensing with Artificial Intelligence (AI)

AI has been extensively studied in both academia and industry for different fields. For wireless communication, an AI/ML TIG was also founded by 802.11 WG in 2022 to study how AI/ML can be combined with 802.11, and 3GPP Release 18 will investigate machine learning (ML) for air interface performance enhancement and overhead reduction. Towards this end, there exist two fields related to IEEE 802.11bf where AI can potentially play an important role.

The first field is the portion that is part of the standard specification. For example, AI-based CSI compression was discussed as a potential solution to reduce feedback overhead for next-generation Wi-Fi standards, which could be reused for Wi-Fi sensing during the CSI matrix feedback. In this regard, generative adversarial net (GAN) [102] could be a potential solution to compress the CSI matrix feedback at the sensing responder and transmit the compressed feedback to the sensing initiator, in which the feedback can be recovered. As the transmitted bits are less and the potential eavesdropper

does not have access to the decoding neural net, the security level could also be improved. With the aid of learning-based solution, the power control during the sensing procedure could also be adapted in real time according to the environment so that more interested sensing results could be obtained. It is also foreseen that different sensing tasks might have different CSI feedback requirements and the feedback requirement for a specific task might change during the whole sensing procedure. Therefore, it is possible that a task-oriented feedback overhead control system could be built based on several AI models such as deep reinforcement learning (DRL) [103], [104], deep neural network (DNN) [105], and long short-term memory (LSTM) [106], so that the sensing performance can be ensured with minimum feedback overhead.

The second field is how to utilize the sensing results to facilitate interesting and innovative WLAN sensing applications. In most indoor scenarios such as smart home and smart factory, a large number of obstacles may exist, leading to NLoS paths in signal propagation. In these scenarios, it is hard to find out the appropriate model to precisely model the channel condition. By contrast, the learning-based method could learn the patterns of the environment from the previous training sets based on the sensing reports and accordingly produce expected prediction in detection, recognition and estimation tasks [9], [107]–[109]. The reconstruction of radio map [110], [111] could also make use of the sensing reports from various nodes so that it could be built based on learning-based methods to facilitate not only sensing, but also communication. Besides, the environment imaging construction could also benefit from WLAN sensing results via ubiquitous deployed WLAN sensing APs. The sensing results for different locations could be combined with the results from other multi-modal non-WLAN devices to possibly build a digital-twin of the corresponding physical objects, landscape, and environment [112], [113]. Furthermore, it is envisioned that with the aid of those techniques from advanced AI models such as large language models (LLMs) [114]–[117], it is possible to use these constructed imaging results to produce artificial images that are originated but quite different from the real environment, i.e., Artificial intelligence generated content (AIGC) [118], which should have wide applications in video games, movie production, house decoration, etc. Last but not least, the WLAN sensing, together with the indoor communication via Wi-Fi, could be combined with the LLMs via properly designed application interfaces (APIs) [119]–[121], which will have broad applications in health care, intelligent home assistant, etc. However, most of these promising directions combined with AI are still at its infant stage and require further investigation for its full maturity.

C. Sensing at Intelligent Edge

As mentioned above, AI plays a significant role in WLAN sensing. Motivated by the development of AI and modern communication and networking technologies, AI services have been pushed from centralized cloud to network edge to reduce the latency and communication cost, which brings about an emerging research area known as edge intelligence [122]–[125]. The realization of edge intelligence depends on two

stages, i.e., edge learning and edge inference. In the following, we discuss the future routine of WLAN sensing on intelligent edge considering the above two stages, respectively.

For edge learning, the training of AI models for sensing applications is uploaded to edge servers for distributed learning to relieve computation and storage burden of edge devices. In such content, federated edge learning (FEEL) has become a hot research topic to address data privacy concerns and support efficient distributed learning at network edges, e.g., Wi-Fi sensing APs. In FEEL, joint communication and computation design is crucial to improve the overall learning performance, particularly in those AI-based Wi-Fi sensing application with heterogeneous data, different channel qualities, and various hardware capabilities among different sensing edge devices [126]. Besides, it is envisioned that future WLAN APs might have to perform both sensing, communication, and computation functionalities during edge learning [127]. This will result in complicated trade-offs among the three entities. Therefore, their joint design for improving the overall performance of WLAN APs' functionality and interoperability is worth pursuing in future work. Second, the service of AI-based sensing tasks may have various goals (e.g., presence detection and body activity detection). Therefore, we need to properly address the joint resource management of sensing, communication, and computation during edge learning in a task-oriented manner, which might even require the new proposal of unique AI model/framework and redesign of learning pipeline tailored for AI-based WLAN sensing applications.

For edge inference, a well-trained model is deployed at network edge for real-time data processing, which is beneficial for AI tasks with stringent latency requirements. Generally, the frameworks of edge inference are categorized as on-device inference [128], on-server inference [129], and split-inference [130]. For on-device and on-server inference, the inference tasks for WLAN sensing are conducted merely on edge devices/servers, which may suffer from limited computation/power resources at devices, as well as communication bottleneck when uploading data to the server. To tackle the above issues, split inference is proposed for edge-device co-inference via deploying AI models on both sides. Furthermore, when multiple Wi-Fi devices cooperate in network sensing, how to design distributed split inference to jointly exploit the distributed wireless sensing data is another interesting but challenging research direction.

Despite the research progress, there are still many open problems for WLAN sensing on edge inference. To start with, how to analyze the inference performance of WLAN sensing on the edge is an important yet challenging problem. Second, with the obtained performance analysis, it is worth pursuing to jointly design the sensing, communication, and computation process to well balance their trade-offs and further improve the overall inference performance. Besides, we might need to train the AI models to do inference in a slightly different way to adapt to the custom environments as the model trained with the datasets from various edge devices might work well on average, but might have poor performance in a specific environment. Finally, with significant volume of WLAN sensing data, it is crucial to extract and transmit their

semantic information in a task-oriented manner to relieve the communication bottleneck for split inference [131], [132].

D. Sensing with Intelligent Reconfigurable Surface (IRS)

Recently, IRS [133], [134] has become a new promising technique for enhancing the wireless communication and sensing performances by configuring the radio propagation environment. Specifically, IRS is a digitally controlled metasurface comprising a larger number of programmable elements. On the one hand, with the smart signal reflection, IRS is able to extend the sensing coverage by creating virtual LoS link to bypass obstacles between transceivers and sensing targets [135], and add extra signal paths towards sensing targets to improve the sensing performance [136]. On the other hand, IRS is also capable of forming the reflective beamforming to enhance the sensing performance at desired regions by properly adjusting the amplitude and/or phase shifts at reflecting elements [137].

First, depending on whether the IRS is composed of a large number of passive reflecting elements or active reflecting elements with signal amplification ability [138], and whether the IRS is deployed with dedicated sensors for receiving and processing target echo signals [137], the IRS-enabled WLAN sensing can be generally implemented based on four different architectures, namely fully-passive IRS sensing, semi-passive IRS self-sensing, active IRS sensing, and active IRS self-sensing. In particular, for the two architectures with passive IRS (i.e., fully-passive IRS sensing and semi-passive IRS self-sensing), the IRS can only reflect the incident signal with desired phase shifts due to the lack of RF chains. While for the two architectures with active IRS (i.e., active IRS sensing and active IRS self-sensing), the active reflecting elements at the IRS is connected to an additional power supply to amplify the amplitude of incident signals, so that combating the severe product-distance path-loss of the reflected channel by IRS. Besides, when the IRS is equipped with dedicated sensors (i.e., semi-passive IRS self-sensing and active IRS self-sensing), the target sensing is implemented at the IRS based on the echo signals through the AP-IRS-target-IRS sensors link. While when there are no any dedicated sensors at the IRS (fully-passive IRS sensing and active IRS sensing), the target sensing is implemented at the AP based on the echo signals through the AP-IRS-target-IRS-AP link.

Then, according to whether the existence of IRS is transparent for the existing WLAN sensing system, there are two different IRS WLAN sensing architectures. For the transparent IRS WLAN sensing architecture, the existing WLAN sensing system does not know the existence of IRS, and thus it completely works based on the existing WLAN sensing protocol. In this case, the IRS adjusts its reflection coefficients by itself. For the non-transparent IRS WLAN sensing architecture, IRS is treated as a new cooperative node in the WLAN sensing system. In this case, the transmit signals at the AP and the reflection coefficients at the IRS are jointly designed, thus information exchange is required between the AP and the IRS. As compared to the transparent counterpart, the non-transparent IRS WLAN sensing can achieve enhanced sensing performance due to the new degrees of freedom provided

by the cooperation of IRS, however, this also requires more complex protocol design.

Despite its great potential, IRS-enabled WLAN sensing still encounters several new challenges. First, the instantaneous CSIs between the AP and the IRS may not be accessible to the AP. In this case, how to design the transmit beamforming at the AP and the reflecting configuration at the IRS based on the long-term channel statistics information is a challenging task. Besides, due to the reflection of IRS, the received echo signals from the target may contain both the direct LoS link and the reflected virtual LoS link, each of which contains different sensing information about the target. In this case, these sensing data from different links should be jointly processed to achieve enhanced sensing performance. Furthermore, with multiple APs and IRSs deployed as a sensing network, the sensing performance could be further enhanced with improved diversity, and its corresponding beamforming and protocol design is a promising research direction.

E. Compatible Technologies for ISAC and Wi-Fi Sensing

In 6G wireless cellular networks, ISAC has been recognized as one of the key attributes [39]. Besides, the mmWave and terahertz (THz) frequency band is envisioned to be utilized in 6G and densely deployed BSs with massive antennas are required to compensate the high path-loss. For example, cell-free massive MIMO and radio stripes have been proposed as a candidate cellular architecture that can be deployed in outdoor and indoor areas such as city squares, cultural places, malls, stadiums, train stations, busy airports, factories, warehouses etc. [139]. However, it is worth noticing that conventional Wi-Fi technology is used to meet the communication requirements of these indoor areas instead. As a result, there is a potential growing tendency that cellular network technology will be closer to WLAN sensing technology in terms of their function, operating frequency band, and deployed environment.

Towards this end, it would be useful to adopt the compatible techniques and designs for both 6G ISAC and WLAN sensing, which will possibly reduce the deployment and implementation cost and also enable cooperative sensing between different APs and small BSs. As cooperative sensing could increase the diversity and gain more information about the sensing targets from multiple facets, this will lead to better sensing performances. For instance, with DMG sensing operating in 60 GHz and mmWave/THz band adopted in future 6G network, the transceivers are very likely to be equipped with massive antennas to form pencil-like directional beams to combat the severe path-loss. Consequently, the potential targets could be located in the near-field or Fresnel region, in which the waveform of the transmitted signal is spherical instead of planar. This new property could be further exploited to enable efficient 3D target localization without stringent synchronization requirements [140], [141], which will benefit both WLAN sensing and ISAC in 6G.

F. Wi-Fi Sensing and ISAC with Wireless Power Transfer (WPT)

As a large number of Internet-of-Things (IoT) devices could be connected to WLAN network and cellular network, there

has been a growing interest in harvesting ambient power such as wireless signal from APs to power these devices. In industry, one of the major milestones is the recent approval of the 802.11 Ambient Power IoT Devices (AMP) SG in March 2023¹², while in academia, simultaneous wireless information and power transfer (SWIPT) has been examined extensively over the past decade [142], which enables the dual use of radio signals for both energy harvesting and communications. Recently, based on previous research endeavors towards SWIPT, researchers start to examine the beamforming and protocol design of multi-functional MIMO system integrating sensing, communication and wireless powering [143]. These three functions could benefit each other, on one hand, with WPT, IoT devices could participate in ISAC seamlessly without its batteries being replaced and recharged manually. On the other, with prior sensing information, the MIMO system could form more accurate beams towards IoT devices, resulting in more efficient energy harvesting and high-quality communication. As such, we believe that the integration of sensing, communications, and powering will be an emerging trend for next-generation WiFi and future 6G.

VIII. CONCLUSION

In this paper, we provided a comprehensive overview of the up-to-date efforts for the emerging IEEE 802.11bf standardization, including the key use cases and the corresponding KPI requirements, WLAN sensing framework and procedure, candidate technical features, evaluation methodology, as well as challenges and future research directions. Specifically, we initially introduced how IEEE 802.11bf was formed and the timeline for its standardization. Next, a detailed literature survey on use cases of WLAN sensing was provided with their KPI requirements specified. Furthermore, we described the sensing procedure used in IEEE 802.11bf to address the sensing measurement acquisition problem for both sub-7GHz sensing and DMG sensing and further discussed their shared features, similarities and differences. We also provided a concrete example to show how sensing task is implemented based on 802.11bf. Then, several key candidate technical features that are likely to be approved in the IEEE 802.11bf were discussed and analyzed. Besides, we elaborated the evaluation methodology, channel modeling, and link-level simulation for the IEEE 802.11bf task group. Finally, several future directions and open challenges that are closely related to the development of IEEE 802.11bf standard and its potential enhancements and applications are discussed. It is our hope that this overview paper can provide useful insights on IEEE 802.11 WLAN sensing for researchers and industrial practitioners to promote its technical advancements and practical deployment.

REFERENCES

[1] Telecom Advisory Services, "The economic value of Wi-Fi: A global view (2021 and 2025)," Telecom Advisory Services, LLC, Tech. Rep., 2021.
 [2] Cognitive. [Online]. Available: <https://www.cognitivesystems.com/>.

[3] Originwireless. [Online]. Available: <https://www.cognitivesystems.com/>.
 [4] S. Yiu, M. Dashti, H. Claussen, and F. Perez-Cruz, "Wireless RSSI fingerprinting localization," *Signal Process.*, vol. 131, pp. 235–244, Feb. 2017.
 [5] Z. Yang, Z. Zhou, and Y. Liu, "From RSSI to CSI: Indoor localization via channel response," *ACM Comput. Surv.*, vol. 46, no. 25, pp. 1–32, 2013.
 [6] F. Zafari, A. Gkelias, and K. K. Leung, "A survey of indoor localization systems and technologies," *IEEE Commun. Surv. Tutor.*, vol. 21, no. 3, pp. 2568–2599, 2019.
 [7] V. Honkavirta, T. Perala, S. Ali-Loytty, and R. Piche, "A comparative survey of WLAN location fingerprinting methods," in *6th WPNC*, 2009, pp. 243–251.
 [8] P. Kumar, L. Reddy, and S. Varma, "Distance measurement and error estimation scheme for RSSI based localization in wireless sensor networks," in *5th IEEE Conf. Wireless Commun. Sensor Netw. (WCNS)*, 2009, pp. 1–4.
 [9] Y. Ma, G. Zhou, and S. Wang, "WiFi sensing with channel state information: A survey," *ACM Comput. Surv.*, vol. 52, no. 3, pp. 1–36, Jun. 2019.
 [10] Z. Yang, Y. Zhang, G. Chi, and G. Zhang, Hands-on wireless sensing with Wi-Fi: A tutorial. [Online]. Available: <https://arxiv.org/abs/2206.09532>.
 [11] L. N. Kandel and S. Yu, "Indoor localization using commodity Wi-Fi APs: techniques and challenges," in *Proc. IEEE Int. Conf. Comput., Netw., and Commun. (ICNC)*, Apr. 2019, pp. 526–530.
 [12] R. Roy and T. Kailath, "ESPRIT-estimation of signal parameters via rotational invariance techniques," *IEEE Trans. Acoust., Speech, Signal Process.*, vol. 37, no. 7, pp. 984–995, Jul. 1989.
 [13] R. Schmidt, "Multiple emitter location and signal parameter estimation," *IEEE Trans. Antennas Propag.*, vol. 34, no. 3, pp. 276–280, Mar. 1986.
 [14] J. A. Fessler and A. O. Hero, "Space-alternating generalized expectation-maximization algorithm," *IEEE Trans. Signal Process.*, vol. 42, no. 10, pp. 2664–2677, Oct. 1994.
 [15] T. Hang, Y. Zheng, K. Qian, C. Wu, Z. Yang, X. Zhou, Y. Liu, and G. Chen, "WiSH: WiFi-based real-time human detection," *Tsinghua Sci. Technol.*, vol. 24, no. 5, pp. 615–629, Oct. 2019.
 [16] D. Vasisht, S. Kumar, and D. Katabi, "Decimeter-level localization with a single WiFi access point," in *Proc. 13th USENIX Symp. Netw. Syst. Design Implement. (NSDI)*, Mar. 2016, pp. 165–178.
 [17] X. Li, D. Zhang, Q. Lv, J. Xiong, S. Li, Y. Zhang, and H. Mei, "Indotrack: Device-free indoor human tracking with commodity Wi-Fi," *ACM Interact. Mob. Wearable Ubiquitous Technol.*, vol. 1, no. 72, pp. 1–22, Sept. 2017.
 [18] X. Liu, J. Cao, S. Tang, and J. Wen, "Wi-Sleep: Contactless sleep monitoring via WiFi signals," in *Proc. IEEE Real-Time Syst. Symp.*, Dec. 2014, pp. 346–355.
 [19] J. Liu, Y. Wang, Y. Chen, J. Yang, X. Chen, and J. Cheng, "Tracking vital signs during sleep leveraging off-the-shelf WiFi," in *16th ACM Int. Symp. Mobile Ad Hoc Netw. Comput.*, Jun. 2015, pp. 267–276.
 [20] X. Wang, C. Yang, and S. Mao, "PhaseBeat: Exploiting CSI phase data for vital sign monitoring with commodity WiFi devices," in *Proc. IEEE 37th Int. Conf. Distrib. Comput. Syst. (ICDCS)*, Jul. 2017, pp. 1230–1239.
 [21] R. Yang, X. Yang, J. Wang, M. Zhou, Z. Tian, and L. Li, "Decimeter level indoor localization using wifi channel state information," *IEEE Sens. J.*, vol. 22, no. 6, pp. 4940–4950, Mar. 2021.
 [22] M. F. Keskin, A. D. Sezer, and S. Gezici, "Localization via visible light systems," *Proc. IEEE*, vol. 106, no. 6, pp. 1063–1088, May. 2018.
 [23] R. Zhang, W.-D. Zhong, K. Qian, S. Zhang, and P. Du, "A reversed visible light multitarget localization system via sparse matrix reconstruction," *IEEE Internet Things J.*, vol. 5, no. 5, pp. 4223–4230, Oct. 2018.
 [24] C.-C. Hsu, H.-C. Chen, and C.-Y. Lai, "An improved ultrasonic-based localization using reflection method," in *Proc. Int. Asia Conf. Informat. Control, Autom. Robot.*, Feb. 2009, pp. 437–440.
 [25] J. Han, C. Qian, X. Wang, D. Ma, J. Zhao, W. Xi, Z. Jiang, and Z. Wang, "Twins: Device-free object tracking using passive tags," *IEEE ACM Trans. Netw.*, vol. 24, no. 2, pp. 1605–1617, Jun. 2016.
 [26] S. Park and S. Hashimoto, "Autonomous mobile robot navigation using passive RFID in indoor environment," *IEEE Trans. Ind. Electron.*, vol. 56, no. 7, pp. 2366–2373, Feb. 2009.
 [27] A. A. N. Shirehijini, A. Yassine, and S. Shirmohammadi, "An RFID-based position and orientation measurement system for mobile objects

¹²Please refer to <https://iee802.org/11/> for its up-to-date progress.

- in intelligent environments,” *IEEE Trans. Instrum. Meas.*, vol. 61, no. 6, pp. 1664–1675, Jan. 2012.
- [28] L. Flueraatoru, S. Wehrli, M. Magno, and D. Niculescu, “On the energy consumption and ranging accuracy of ultra-wideband physical interfaces,” in *Proc. IEEE Global Commun. Conf. (GLOBECOM)*, Dec. 2020, pp. 1–7.
- [29] Y.-H. Ho, G.-H. Hou, M.-H. Wu, F.-H. Chen, P.-S. Sung, C.-H. Chen, and C.-L. Lin, “High-precision UWB indoor positioning system for customer pathway tracking,” in *Proc. IEEE 8th Global Conf. Consum. Electron. (GCCE)*, Oct. 2019, pp. 466–467.
- [30] A. Mackey, P. Spachos, L. Song, and K. N. Plataniotis, “Improving BLE beacon proximity estimation accuracy through bayesian filtering,” *IEEE Internet Things J.*, vol. 7, no. 4, pp. 3160–3169, Jan. 2020.
- [31] M. F. Keskin, A. D. Sezer, and S. Gezici, “Towards a visible light network architecture for continuous communication and localization,” in *ACM VLCS*, Oct. 2016, pp. 49–54.
- [32] S. Zhu and X. Zhang, “Enabling high-precision visible light localization in today’s buildings,” in *ACM MobiSys*, Jun. 2017, pp. 96–108.
- [33] X. Luo, H. Wang, S. Yan, J. Liu, Y. Zhong, and R. Lan, “Ultrasonic localization method based on receiver array optimization schemes,” *Int. J. Distrib. Sens. Netw.*, vol. 14, no. 11, Nov. 2018.
- [34] Q. Lin, Z. An, and L. Yang, “Rebooting ultrasonic positioning systems for ultrasound-incapable smart devices,” in *ACM MobiSys*, Aug. 2019, pp. 1–16.
- [35] A. Motroni, A. Buffi, and P. Nepa, “A survey on indoor vehicle localization through RFID technology,” *IEEE Access*, vol. 9, pp. 17 921–17 942, Jan. 2021.
- [36] A. Alarifi, A. Al-Salman, M. Alsaleh, A. Alnafessah, S. Al-Hadhrani, M. Al-Ammar, and H. S. Al-Khalifa, “Ultra wideband indoor positioning technologies: Analysis and recent advances,” *Sensors*, vol. 16, no. 5, pp. 707–743, May 2016.
- [37] Y. Chen, J. Zhang, W. Feng, and M.-S. Alouini, “Radio sensing using 5G signals: Concepts, state of the art, and challenges,” *IEEE Internet Things J.*, vol. 9, no. 2, pp. 1037–1052, Dec. 2021.
- [38] X. Yang, D. Fan, A. Ren, N. Zhao, and M. Alam, “5G-based user-centric sensing at C-band,” *IEEE Trans. Industr. Inform.*, vol. 15, no. 5, pp. 3040–3047, Jan. 2019.
- [39] ITU-R WP5D, “IMT-framework for 2030 and beyond,” Feb. 2023. [Online]. Available: https://www.itu.int/dms_ties/itu-r/md/19/wp5d/c/R19-WP5D-C-1668/H3-N3.07/MSW-E.docx
- [40] Linux 802.11n CSI Tool. [Online]. Available: <https://dhalperi.github.io/linux-80211n-csitol/>.
- [41] Atheros-CSI-Tool. [Online]. Available: <https://wands.sg/research/wifi/AtherosCSI/Hardware.html>.
- [42] Y. Xie, Z. Li, and M. Li, “Precise power delay profiling with commodity Wi-Fi,” *IEEE Trans. Mob. Comput.*, vol. 18, no. 6, pp. 1342–1355, Jun. 2019.
- [43] F. Liu, Y. Cui, C. Masouros, J. Xu, T. X. Han, Y. C. Eldar, and S. Buzzi, “Integrated sensing and communications: Towards dual-functional wireless networks for 6G and beyond,” *IEEE J. Sel. Areas Commun.*, vol. 40, no. 6, pp. 1728–1767, Jun. 2022.
- [44] H. Hua, T. X. Han, and J. Xu, “MIMO integrated sensing and communication: CRB-rate tradeoff,” *IEEE Trans. Wireless Commun.*, pp. 1–1, Aug. 2023.
- [45] H. Hua, J. Xu, and T. X. Han, “Optimal transmit beamforming for integrated sensing and communication,” *IEEE Trans. Veh. Technol.*, vol. 72, no. 8, pp. 10 588–10 603, Mar. 2023.
- [46] Z. Lyu, G. Zhu, and J. Xu, “Joint maneuver and beamforming design for UAV-enabled integrated sensing and communication,” *IEEE Trans. Wireless Commun.*, vol. 22, no. 4, pp. 2424–2440, Apr. 2022.
- [47] X. Song, X. Qin, J. Xu, and R. Zhang, “Cramér-Rao bound minimization for IRS-enabled multiuser integrated sensing and communication,” Jun. 2023. [Online]. Available: <https://arxiv.org/pdf/2306.17493.pdf>
- [48] X. Song, D. Zhao, H. Hua, T. X. Han, X. Yang, and J. Xu, “Joint transmit and reflective beamforming for IRS-assisted integrated sensing and communication,” in *Proc. IEEE WCNC*, Austin, TX, USA, May 2022, pp. 189–194.
- [49] J. Segev, P. Thornycroft, D. Stanley, Q. Wang, B. Hart, S. Pandey, N. Kakani, J. Roshdahl, G. Venkatesan, L. Chu, E. Au, G. Bajko, C. Wang, M. Rison, F. Tang, C. Aldana, P. Dua, and M. Wang. Ngp par draft. 2015, Jul. [Online]. Available: <https://mentor.ieee.org/802.11/dcn/15/11-15-0030-09-0ngp-ngp-par-draft.docx>.
- [50] C. Chen, H. Song, Q. Li, F. Meneghello, F. Restuccia, and C. Cordeiro, “Wi-Fi sensing based on IEEE 802.11 bf,” *IEEE Commun. Mag.*, vol. 61, no. 1, pp. 121–127, Nov. 2022.
- [51] S. Blandino, T. Ropitault, C. R. da Silva, A. Sahoo, and N. Golmie, “IEEE 802.11 bf DMG sensing: Enabling high-resolution mmwave Wi-Fi sensing,” *IEEE Open J. Veh. Technol.*, vol. 4, pp. 342–355, Jan. 2023.
- [52] F. Meneghello, C. Chen, C. Cordeiro, and F. Restuccia, “Toward integrated sensing and communications in IEEE 802.11 bf Wi-Fi networks,” *IEEE Commun. Mag.*, vol. 61, no. 7, pp. 128–133, Jul. 2023.
- [53] T. X. Han, R. Du, C. Liu, M. Zhang, and D. X. Yang. Wi-fi sensing. [Online]. Available: <https://mentor.ieee.org/802.11/dcn/19/11-19-1164-00-0wng-wi-fi-sensing.pptx>.
- [54] C. da Silva, C. Cordeiro, B. Sadeghi, C. Chen, and A. Lomayev. Wi-fi sensing: Usages, requirements, technical feasibility and standards gaps. 2019, Jul. [Online]. Available: [IEEE802.11-19/1293r0](https://mentor.ieee.org/802.11-19/1293r0).
- [55] T. X. Han, R. Du, B. Zhou, X. Peng, Z. Rong, P. Zhang, J. Luo, C. Liu, M. Zhang, D. Shang, J. Li, D. X. Yang, X. Zuo, K. Meng, G. X. Hu, and X. Dong. Wi-fi sensing - follow up. 2019, Jul. [Online]. Available: [IEEE802.11-19/1500r0](https://mentor.ieee.org/802.11-19/1500r0).
- [56] IEEE 802.11. Status of IEEE 802.11 WLAN Sensing (SENS) SG. [Online]. Available: https://www.ieee802.org/11/Reports/senstig_S_Update.htm.
- [57] IEEE, “IEEE standard for information technology–telecommunications and information exchange between systems – local and metropolitan area networks–specific requirements – part 11: Wireless LAN medium access control (MAC) and physical layer (PHY) specifications,” IEEE Std 802.11-2020 (Revision of IEEE Std 802.11-2016), Tech. Rep., 2021.
- [58] C. Silva. 802.11 SENS SG Proposed PAR. 2020, Aug. [Online]. Available: [IEEE802.11-19/2103r12](https://mentor.ieee.org/802.11-19/2103r12).
- [59] Y. Sun, D. K. P. Tan, R. Du, C. Liu, M. Zhang, and E. Au. Usage model terminology for WLAN sensing. 2020, Jun. [Online]. Available: <https://mentor.ieee.org/802.11/dcn/20/11-20-0905-02-SENS-usage-model-terminology-for-wlan-sensing.pptx>.
- [60] A. Kasher, A. Eitan, S. Trainin, Y. Sun, and R. Du. WiFi sensing use cases. 2021, Jan. [Online]. Available: <https://mentor.ieee.org/802.11/dcn/20/11-20-1712-02-00bf-wifi-sensing-use-cases.xlsx>.
- [61] K. J. R. Liu and B. Wang. *Wireless AI: Wireless sensing, positioning, IoT, and communications*. Cambridge, U.K.: Cambridge Univ., 2019.
- [62] D. Zhang, D. Wu, K. Niu, X. Wang, F. Zhang, J. Yao, D. Jiang, and F. Qin, “Practical issues and challenges in CSI-based integrated sensing and communication,” in *Proc. IEEE Int. Conf. Commun. Workshops (ICC Workshops)*, Jul. 2022, pp. 836–841.
- [63] D. K. P. Tan, R. Du, Y. Sun, T. X. Han, D. X. Yang, W. Tong, W. Ding, Y. Li, and Y. Zhang, “Wi-Sneeze- Sneeze sensing using Wi-Fi signals,” in *Proc. IEEE Globecom Workshops (GC Wkshps)*, Dec. 2020, pp. 1–6.
- [64] OpenPose. [Online]. Available: <https://github.com/CMU-Perceptual-Computing-Lab/openpose>.
- [65] C. B. Barneto, E. Rastorgueva-Foi, M. F. Keskin, T. Riihonen, M. Turunen, J. Talvitie, H. Wymeersch, and M. Valkama, “Millimeter-wave mobile sensing and environment mapping: Models, algorithms and validation,” *IEEE Trans. Veh. Technol.*, vol. 71, no. 4, pp. 3900–3916, Jan. 2022.
- [66] E. Leitinger, F. Meyer, F. Hlawatsch, K. Witrisal, F. Tufvesson, and M. Z. Win, “A belief propagation algorithm for multipath-based SLAM,” *IEEE Trans. Wireless Commun.*, vol. 18, no. 12, pp. 5613–5629, Sept. 2019.
- [67] M. Zhao, Y. Tian, H. Zhao, M. A. Alsheikh, T. Li, R. Hristov, Z. Kabelac, D. Katabi, and A. Torralba, “RF-based 3D skeletons,” in *Proc. Conf. ACM Special Interest Group Data Commun.*, Aug. 2018, pp. 267–281.
- [68] F. Wang, S. Zhou, S. Panev, J. Han, and D. Huang, “Person-in-WiFi: Fine-grained person perception using WiFi,” in *Proc. IEEE/CVF Int. Conf. Comput. Vis. (ICCV)*, Oct. 2019, pp. 5452–5461.
- [69] W. Jiang, H. Xue, C. Miao, S. Wang, S. Lin, C. Tian, S. Murali, H. Hu, Z. Sun, and L. Su, “Towards 3D human pose construction using WiFi,” in *Proc. 26th Annual Int. Conf. Mobile Comput. and Netw.*, Apr. 2020, pp. 1–14.
- [70] C. Chen, D. Das, and C. Cordeiro. Non-tb sensing measurement. 2021, Aug. [Online]. Available: <https://mentor.ieee.org/802.11/dcn/21/11-21-1433-02-00bf-non-tb-sensing-measurement.pptx>.
- [71] Narengerile, R. Du, M. Hu, Y. Xin, and A. Kasher. Dmg passive sensing based on a-bft. 2021, Mar. [Online]. Available: <https://mentor.ieee.org/802.11/dcn/22/11-22-0423-00-00bf-dmg-passive-sensing-based-on-a-bft.pptx>.
- [72] R. Du, D. T. K. Pin, M. Zhang, C. Liu, and Y. Sun. Discussion on WLAN sensing sequence design-follow up. 2020, Sep. [On-

- line]. Available: <https://mentor.ieee.org/802.11/dcn/20/11-20-1529-00-SENS-discussion-on-wlan-sensing-sequence-design-follow-up.pptx>.
- [73] M. I. Skolnik, *Introduction to radar systems*. New York, 1980.
- [74] IEEE, "Enhanced throughput for operation in license-exempt bands above 45 GHz," IEEE 802.11 Working Group, Tech. Rep., 2017.
- [75] B. Farhang-Boroujeny, "OFDM versus filter bank multicarrier," *IEEE Signal Process. Mag.*, vol. 28, no. 3, pp. 92–112, Apr. 2011.
- [76] Z. Ye, Z. Zhou, P. Fan, Z. Liu, X. Lei, and X. Tang, "Low ambiguity zone: Theoretical bounds and doppler-resilient sequence design in integrated sensing and communication systems," *IEEE J. Sel. Areas Commun.*, vol. 40, no. 6, pp. 1809–1822, Mar. 2022.
- [77] A. Kasher. PDT EDMG multi-static PPDU structure. 2022, Mar. [Online]. Available: <https://mentor.ieee.org/802.11/dcn/22/11-22-0464-06-00bf-pdt-edmg-multi-static-ppdu-structure.docx>.
- [78] R. Chitrakar, R. Pushkarna, Y. Ding, Y. Urabe, and H. Motozuka. Partial CSI feedback. 2021, Nov. [Online]. Available: <https://mentor.ieee.org/802.11/dcn/21/11-21-1921-01-00bf-partial-csi-feedback.pptx>.
- [79] R. Du, C. Liu, M. Zhang, Y. Sun, and D. K. P. Tan. Truncated power delay profile. 2021, May. [Online]. Available: <https://mentor.ieee.org/802.11/dcn/21/11-21-0660-00-00bf-truncated-power-delay-profile.pptx>.
- [80] Q. Li, H. Song, X. Chen, C. Chen, and R. Stacey. PDT EDMG multi-static PPDU structure. 2022, Mar. [Online]. Available: <https://mentor.ieee.org/802.11/dcn/22/11-22-0506-01-00bf-differential-quantization-for-csi-report.pptx>.
- [81] A. Eitan, A. Kasher, and S. Trainin. Imaging radar data report. 2021, Nov. [Online]. Available: <https://mentor.ieee.org/802.11/dcn/21/11-21-1801-02-00bf-imaging-radar-data-report.pptx>.
- [82] IEEE, "IEEE standard for information technology-telecommunications and information exchange between systems-local and metropolitan area networks-specific requirements part 11 : Wireless LAN medium access control (MAC) and physical layer (PHY) specifications." IEEE 802.11 Working Group, Tech. Rep., 2012.
- [83] J. Suh, Y. Xin, O. AboulMagd, and E. Au. Simplified scaling factor feedback for CSI matrices quantization. 2021, Oct. [Online]. Available: <https://mentor.ieee.org/802.11/dcn/21/11-21-1676-01-00bf-simplified-scaling-factor-feedback-for-csi-matrices.pptx>.
- [84] S. Shellhammer, B. Tian, A. Raissinia, and S. Merlin. Simplified scaling factor feedback for CSI matrices quantization. 2021, Oct. [Online]. Available: <https://mentor.ieee.org/802.11/dcn/21/11-21-1573-01-00bf-low-complexity-scaling-and-quantization-for-csi-report.pptx>.
- [85] M. Montemurro. Sensing security requirements. 2022, Apr. [Online]. Available: <https://mentor.ieee.org/802.11/dcn/22/11-22-0401-04-00bf-sensing-security-requirements.pptx>.
- [86] R. Du, M. Zhang, Y. Lv, M. Hu, K. S. Au, Y. Xin, J. Suh, O. AboulMagd, H. Dai, S. Shi, W. Wang, Y. Shen, J. Xu, and F. Liu. 11bf evaluation methodology and simulation scenarios. 2021, Sep. [Online]. Available: <https://mentor.ieee.org/802.11/dcn/21/11-21-0876-03-00bf-11bf-evaluation-methodology-and-simulation-scenarios.doc>.
- [87] M. Zhang. Channel models for WLAN sensing systems. 2021, Aug. [Online]. Available: <https://mentor.ieee.org/802.11/dcn/21/11-21-0782-03-00bf-channel-models-for-wlan-sensing-systems.docx>.
- [88] R. Du, M. Zhang, C. Liu, Y. Sun, D. K. P. Tan, and E. Au. Discussion on WLAN sensing evaluation methodology. 2020, Jul. [Online]. Available: <https://mentor.ieee.org/802.11/dcn/20/11-20-0907-01-SENS-discussion-on-wlan-sensing-evaluation-methodology.pptx>.
- [89] R. Porat. Evaluation methodology. 2016, Jan. [Online]. Available: <https://mentor.ieee.org/802.11/dcn/14/11-14-0571-12-00ax-evaluation-methodology.docx>.
- [90] L. Cariou. 11ay evaluation methodology. 2016, May. [Online]. Available: <https://mentor.ieee.org/802.11/dcn/15/11-15-0866-04-00ay-11ay-evaluation-methodology.doc>.
- [91] M. Zhang, R. Du, X. Peng, C. Liu, Y. Sun, D. K. Tan, R. Wang, S. Wang, and X. Li. Discussion of channel model for WLAN sensing. 2020, Jun. [Online]. Available: <https://mentor.ieee.org/802.11/dcn/20/11-20-0906-00-SENS-discussion-of-channel-model-for-wlan-sensing.pptx>.
- [92] J. Liu. TGax channel model document. 2014, Sep. [Online]. Available: <https://mentor.ieee.org/802.11/dcn/14/11-14-0882-04-00ax-tgax-channel-model-document.docx>.
- [93] A. Maltsev. Channel models for IEEE 802 11ay. 2017, Mar. [Online]. Available: <https://mentor.ieee.org/802.11/dcn/15/11-15-1150-09-00ay-channel-models-for-ieee-802-11ay.docx>.
- [94] Z. Yun and M. F. Iskander, "Ray tracing for radio propagation modeling: Principles and applications," *IEEE Access*, vol. 3, pp. 1089–1100, Jul. 2015.
- [95] Y. Lv, X. Peng, R. Du, M. Hu, H. Xie, R. Wang, S. Wang, Z. Zang, and G. Li. Channel models for WLAN sensing systems. 2021, Jul. [Online]. Available: <https://mentor.ieee.org/802.11/dcn/21/11-21-1241-00-00bf-data-driving-hybrid-channel-model-for-wlan-sensing.pptx>.
- [96] G. Li, S. Wang, J. Li, R. Wang, F. Liu, M. Zhang, X. Peng, and T. X. Han. (Jul. 2021) Rethinking the tradeoff in integrated sensing and communication: Recognition accuracy versus communication rate. [Online]. Available: <https://arxiv.org/abs/2107.09621>.
- [97] R. Du, M. Zhang, C. Liu, Y. Sun, D. T. K. Pin, and A. E. WLAN sensing link level simulation. 2020, Oct. [Online]. Available: <https://mentor.ieee.org/802.11/dcn/20/11-20-1642-00-00bf-wlan-sensing-link-level-simulation.pptx>.
- [98] R. Du, M. Zhang, X. Peng, D. K. P. Tan, C. Liu, Y. Sun, H. Dai, S. Shi, and W. Wang. WLAN sensing link level simulation - follow ups. 2021, Mar. [Online]. Available: <https://mentor.ieee.org/802.11/dcn/21/11-21-0352-01-00bf-wlan-sensing-link-level-simulation-follow-ups.pptx>.
- [99] M. Hu, Z. Mao, M. Gan, B. Gang, X. Liu, X. Bai, R. Yu, Y. Xin, and G. Tsodik. Thoughts on utilizing mmwave. 2022, Mar. [Online]. Available: <https://mentor.ieee.org/802.11/dcn/23/11-23-0066-02-0uhr-thoughts-on-utilizing-mmwave.pptx>.
- [100] E. Park, D. Lim, J. Chun, and J. Choi. Considerations on PHY designs for mmwave band. 2022, Nov. [Online]. Available: <https://mentor.ieee.org/802.11/dcn/22/11-22-1872-00-0uhr-considerations-on-phy-designs-for-mmwave-band.pptx>.
- [101] L. Cariou, R. Stacey, and C. Cordeiro. mmwave operation in uhr. 2022, Nov. [Online]. Available: <https://mentor.ieee.org/802.11/dcn/22/11-22-1884-00-0uhr-mmwave-operation-for-uhr.pptx>.
- [102] I. Goodfellow, J. Pouget-Abadie, M. Mirza, B. Xu, D. Warde-Farley, S. Ozair, A. Courville, and Y. Bengio, "Generative adversarial networks," *Commun. ACM*, vol. 63, no. 11, pp. 139–144, Nov. 2020.
- [103] K. Arulkumaran, M. P. Deisenroth, M. Brundage, and A. A. Bharath, "Deep reinforcement learning: A brief survey," *IEEE Signal Process. Mag.*, vol. 34, no. 6, pp. 26–38, Nov. 2017.
- [104] N. C. Luong, D. T. Hoang, S. Gong, D. Niyato, P. Wang, Y.-C. Liang, and D. I. Kim, "Applications of deep reinforcement learning in communications and networking: A survey," *IEEE Commun. Surv. Tutor.*, vol. 21, no. 4, pp. 3133–3174, May 2019.
- [105] Y. LeCun, Y. Bengio, and G. Hinton, "Deep learning," *Nature*, vol. 521, no. 7553, pp. 436–444, May 2015.
- [106] S. Hochreiter and J. Schmidhuber, "Long short-term memory," *Neural computation*, vol. 9, no. 8, pp. 1735–1780, Nov. 1997.
- [107] M. A. Alsheikh, S. Lin, D. Niyato, and H.-P. Tan, "Machine learning in wireless sensor networks: Algorithms, strategies, and applications," *IEEE Commun. Surv. Tutor.*, vol. 16, no. 4, pp. 1996–2018, Apr. 2014.
- [108] R. Zhou, X. Lu, P. Zhao, and J. Chen, "Device-free presence detection and localization with SVM and CSI fingerprinting," *IEEE Sens. J.*, vol. 17, no. 23, pp. 7990–7999, Oct. 2017.
- [109] K. Ohara, T. Maekawa, and Y. Matsushita, "Detecting state changes of indoor everyday objects using Wi-Fi channel state information," *Proc. ACM on Interact. Mob. Wearable Ubiquitous Technol.*, vol. 1, no. 3, pp. 1–28, Sept. 2017.
- [110] R. Levie, Ç. Yapar, G. Kutyniok, and G. Caire, "Radiounet: Fast radio map estimation with convolutional neural networks," *IEEE Trans. Wireless Commun.*, vol. 20, no. 6, pp. 4001–4015, Feb. 2021.
- [111] Y. Zeng, J. Chen, J. Xu, D. Wu, X. Xu, S. Jin, X. Gao, D. Gesbert, S. Cui, and R. Zhang, "A tutorial on environment-aware communications via channel knowledge map for 6G," *arXiv preprint arXiv:2309.07460*, Sept. 2023.
- [112] F. Tao, H. Zhang, A. Liu, and A. Y. Nee, "Digital twin in industry: State-of-the-art," *IEEE Trans. Ind. Inform.*, vol. 15, no. 4, pp. 2405–2415, Sept. 2018.
- [113] A. Fuller, Z. Fan, C. Day, and C. Barlow, "Digital twin: Enabling technologies, challenges and open research," *IEEE Access*, vol. 8, pp. 108952–108971, May 2020.
- [114] A. Chowdhery, S. Narang, J. Devlin, M. Bosma, G. Mishra, A. Roberts, P. Barham, H. W. Chung, C. Sutton, S. Gehrmann *et al.*, "Palm: Scaling language modeling with pathways," *arXiv preprint arXiv:2204.02311*, Apr. 2022.
- [115] A. Vaswani, N. Shazeer, N. Parmar, J. Uszkoreit, L. Jones, A. N. Gomez, Ł. Kaiser, and I. Polosukhin, "Attention is all you need," *Adv. Neural Inf. Process.*, vol. 30, Dec. 2017.
- [116] H. W. Chung, L. Hou, S. Longpre, B. Zoph, Y. Tay, W. Fedus, E. Li, X. Wang, M. Dehghani, S. Brahma *et al.*, "Scaling instruction-finetuned language models," *arXiv preprint arXiv:2210.11416*, Oct. 2022.
- [117] J. Hoffmann, S. Borgeaud, A. Mensch, E. Buchatskaya, T. Cai, E. Rutherford, D. d. L. Casas, L. A. Hendricks, J. Welbl, A. Clark *et al.*,

- “Training compute-optimal large language models,” *arXiv preprint arXiv:2203.15556*, Mar. 2022.
- [118] Y. Cao, S. Li, Y. Liu, Z. Yan, Y. Dai, P. S. Yu, and L. Sun, “A comprehensive survey of AI-generated content (AIGC): A history of generative AI from GAN to ChatGPT,” *arXiv preprint arXiv:2303.04226*, Mar. 2023.
- [119] P. Lewis, E. Perez, A. Piktus, F. Petroni, V. Karpukhin, N. Goyal, H. Küttler, M. Lewis, W.-t. Yih, T. Rocktäschel *et al.*, “Retrieval-augmented generation for knowledge-intensive NLP tasks,” *Adv. Neural Inf. Process.*, vol. 33, pp. 9459–9474, Dec. 2020.
- [120] L. Gao, A. Madaan, S. Zhou, U. Alon, P. Liu, Y. Yang, J. Callan, and G. Neubig, “PAL: Program-aided language models,” in *ICML*. PMLR, 2023, pp. 10764–10799.
- [121] S. Yao, J. Zhao, D. Yu, N. Du, I. Shafran, K. Narasimhan, and Y. Cao, “React: Synergizing reasoning and acting in language models,” *arXiv preprint arXiv:2210.03629*, Oct. 2022.
- [122] G. Zhu, Z. Lyu, X. Jiao, P. Liu, M. Chen, J. Xu, S. Cui, and P. Zhang, “Pushing AI to wireless network edge: An overview on integrated sensing, communication, and computation towards 6G,” *Sci. China Inf. Sci.*, vol. 66, no. 130301, pp. 1–19, Feb. 2023.
- [123] L. Chang, Z. Zhang, P. Li, S. Xi, W. Guo, Y. Shen, Z. Xiong, J. Kang, D. Niyato, X. Qiao *et al.*, “6G-enabled edge AI for metaverse: Challenges, methods, and future research directions,” *J. commun. inf. netw.*, vol. 7, no. 2, pp. 107–121, Jun. 2022.
- [124] W. Y. B. Lim, N. C. Luong, D. T. Hoang, Y. Jiao, Y.-C. Liang, Q. Yang, D. Niyato, and C. Miao, “Federated learning in mobile edge networks: A comprehensive survey,” *IEEE Commun. Surv. Tutor.*, vol. 22, no. 3, pp. 2031–2063, Apr. 2020.
- [125] X. Wang, Y. Han, V. C. Leung, D. Niyato, X. Yan, and X. Chen, “Convergence of edge computing and deep learning: A comprehensive survey,” *IEEE Commun. Surv. Tutor.*, vol. 22, no. 2, pp. 869–904, Jan. 2020.
- [126] M. Chen, Z. Yang, W. Saad, C. Yin, H. V. Poor, and S. Cui, “A joint learning and communications framework for federated learning over wireless networks,” *IEEE Trans. Wireless Commun.*, vol. 20, no. 1, pp. 269–283, Jan. 2020.
- [127] D. Wen, P. Liu, G. Zhu, Y. Shi, J. Xu, Y. C. Eldar, and S. Cui, “Task-oriented sensing, computation, and communication integration for multi-device edge AI,” *IEEE Trans. Wireless Commun.*, Aug. 2023.
- [128] S. F. Yilmaz, B. Hasircioğlu, and D. Gündüz, “Over-the-air ensemble inference with model privacy,” in *Proc. IEEE Int. Symp. Inf. Theory*, Jul. 2022, pp. 1265–1270.
- [129] K. Yang, Y. Shi, W. Yu, and Z. Ding, “Energy-efficient processing and robust wireless cooperative transmission for edge inference,” *IEEE Internet Things J.*, vol. 7, no. 10, pp. 9456–9470, Oct. 2020.
- [130] Z. Liu, Q. Lan, and K. Huang, “Resource allocation for multiuser edge inference with batching and early exiting,” *IEEE J. Sel. Areas Commun.*, vol. 41, no. 4, pp. 1186–1200, Apr. 2023.
- [131] Z. Lyu, G. Zhu, J. Xu, B. Ai, and S. Cui, “Semantic communications for image recovery and classification via deep joint source and channel coding,” Apr. 2023. [Online]. Available: <https://arxiv.org/pdf/2304.02317.pdf>
- [132] J. Shao, Y. Mao, and J. Zhang, “Task-oriented communication for multi-device cooperative edge inference,” *IEEE Trans. Wireless Commun.*, vol. 22, no. 1, pp. 73–87, Jan. 2022.
- [133] Q. Wu, S. Zhang, B. Zheng, C. You, and R. Zhang, “Intelligent reflecting surface-aided wireless communications: A tutorial,” *IEEE Trans. Commun.*, vol. 69, no. 5, pp. 3313–3351, May 2021.
- [134] S. Gong, X. Lu, D. T. Hoang, D. Niyato, L. Shu, D. I. Kim, and Y.-C. Liang, “Toward smart wireless communications via intelligent reflecting surfaces: A contemporary survey,” *IEEE Commun. Surv. Tutor.*, vol. 22, no. 4, pp. 2283–2314, Jun. 2020.
- [135] X. Song, J. Xu, F. Liu, T. X. Han, and Y. C. Eldar, “Intelligent reflecting surface enabled sensing: Cramér-Rao bound optimization,” *IEEE Trans. Signal Process.*, vol. 71, pp. 2011–2026, May 2023.
- [136] S. Buzzi, E. Grossi, M. Lops, and L. Venturino, “Foundations of MIMO radar detection aided by reconfigurable intelligent surfaces,” *IEEE Trans. Signal Process.*, vol. 70, pp. 1749–1763, Mar. 2022.
- [137] X. Song, X. Li, X. Qin, and J. Xu, “Fully-passive versus semi-passive IRS-enabled sensing: SNR analysis,” Aug. 2023. [Online]. Available: <https://arxiv.org/pdf/2308.05420.pdf>
- [138] Z. Kang, C. You, and R. Zhang, “Active-passive IRS aided wireless communication: New hybrid architecture and elements allocation optimization,” *IEEE Trans. Wireless Commun.*, early access, Aug. 2023, doi: 10.1109/TWC.2023.3308373.
- [139] H. Q. Ngo, A. Ashikhmin, H. Yang, E. G. Larsson, and T. L. Marzetta, “Cell-free massive MIMO versus small cells,” *IEEE Trans. Wireless Commun.*, vol. 16, no. 3, pp. 1834–1850, Jan. 2017.
- [140] L. Khamidullina, I. Podkurkov, and M. Haardt, “Conditional and unconditional Cramér-Rao bounds for near-field localization in bistatic MIMO radar systems,” *IEEE Trans. Signal Process.*, vol. 69, pp. 3220–3234, May 2021.
- [141] H. Hua, J. Xu, and Y. C. Eldar, “Near-field 3D localization via MIMO radar: Cramér-Rao bound analysis and estimator design,” *arXiv preprint arXiv:2308.16130*, Aug. 2023.
- [142] B. Clerckx, R. Zhang, R. Schober, D. W. K. Ng, D. I. Kim, and H. V. Poor, “Fundamentals of wireless information and power transfer: From RF energy harvester models to signal and system designs,” *IEEE J. Sel. Areas Commun.*, vol. 37, no. 1, pp. 4–33, 2018.
- [143] Y. Chen, H. Hua, J. Xu, and D. W. K. Ng, “ISAC meets SWIPT: Multi-functional wireless systems integrating sensing, communication, and powering,” *arXiv preprint arXiv:2211.10605*, Aug. 2022.